POGO SUPPRESSION ON THE DELTA VEHICLE

J. G. Payne, et al

Aerospace Corporation

Prepared for:

Space and Missile Systems Organization

7 June 1974

REPORT SAMSO-TR-74-187

Pogo Suppression on the Delta Vehicle

J. G. PAYNE and S. RUBIN
Engineering Science Operations
The Aerospace Corporation
El Segundo, Calif. 90245

7 June 1974

Interim Report

Prepared for

NASA/GODDARD SPACE FLIGHT CENTER
Greenbelt, Maryland 20771

SPACE AND MISSILE SYSTEMS ORGANIZATION
AIR FORCE SYSTEMS COMMAND
Los Angeles Air Force Station
Los Angeles, Calif. 90045

UNCLASSIFIED

SECURITY CLASSIFICATION OF THIS PAGE (When Data Entered)

REPORT DOCUMENTATION PAGE		READ INSTRUCTIONS BEFORE COMPLETING FORM
1 REPORT NUMBER SAMSO-TR-74-187	2. GOVT ACCESSION NO.	3. RECIPIENT'S CATALOG NUMBER
4 TITLE (and Subtitle) Pogo Suppression on the Delta Vehicle		5. TYPE OF REPORT & PERIOD COVERED Interim Jan. 1972-Nov. 1973 6. PERFORMING ORG. REPORT NUMBER TR-0074(4704)-1
7. AUTHOR(s) J. G. Payne and S. Rubin		8. CONTRACT OR GRANT NUMBER(s) F04701-73-C-0074
9. PERFORMING ORGANIZATION NAME AND ADDRESS The Aerospace Corporation El Segundo, California		10. PROGRAM ELEMENT, PROJECT, TASK AREA & WORK UNIT NUMBERS
11. CONTROLLING OFFICE NAME AND ADDRESS Space & Missile Systems Organization Air Force Systems Command Los Angeles Air Force Station Los Angeles, California		12. REPORT DATE 7 June 1974 13. NUMBER OF PAGES 61
14 MONITORING AGENCY NAME & ADDRESS(if different from Controlling Office)		15. SECURITY CLASS. (of this report) Unclassified 15a. DECLASSIFICATION/DOWNGRADING SCHEDULE

16. DISTRIBUTION STATEMENT (of this Report)

A: Approved for public release; distribution unlimited.

17. DISTRIBUTION STATEMENT (of the abstract entered in Block 20, if different from Report)

18. SUPPLEMENTARY NOTES

19. KEY WORDS (Continue on reverse side if necessary and identify by block number)

Pogo	Thor Vehicle
Delta Vehicle	Suppression
Stability	Mathematical Modeling
Accumulator, Resistive	Flight Data Reduction
	Spectral Analyses

20 ABSTRACT (Continue on reverse side if necessary and identify by block number)

A long succession of Delta vehicles (including their Thor/Delta and Thor/Agena predecessors) have experienced pogo instability in the twenty seconds prior to cutoff of the first stage. The study reported here led to the suppression of this instability on the ITOS-F vehicle launched in November 1973.

DD FORM 1473 FACSIMILE

UNCLASSIFIED

SECURITY CLASSIFICATION OF THIS PAGE (When Data Entered)

20. Abstract (Continued)

Suppression was achieved by the addition of flow resistance to an existing accumulator installed in the lox suction line.

The ability to achieve the suppression resulted from a joint study by The Aerospace Corporation and McDonnell Douglas Astronautics Corporation. The study was designed to develop a pogo stability model yielding eigenvalues and eigenvectors consistent with flight data over a range of vehicle configurations, engine operating conditions, and presence or absence of a lox accumulator. Extensive reduction of flight data in the form of spectral analyses was required. Based on this model, it was possible to optimize the accumulator resistance for vehicle stability.

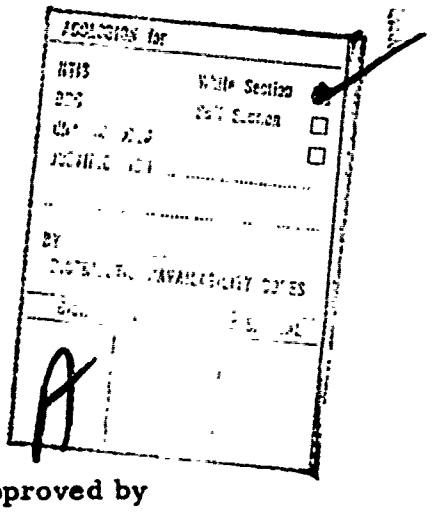

Approved by

S. Rubin

S. Rubin, Senior Staff Engineer
Vehicle Integrity Subdivision
Vehicle Engineering Division

Publication of this report does not constitute Air Force approval of the report's findings or conclusions. It is published only for the exchange and stimulation of ideas.

William D. Knox

William D. Knox, Colonel, USAF
Asst Program Director
Expendable Launch Vehicles SPO

CONTENTS

FIGURES

FIGURES (Continued)

SECTION I

INTRODUCTION

Since February 1972 The Aerospace Corporation has been involved in a joint study with the McDonnell Douglas Astronautics Corporation (MDAC) in an effort to suppress pogo oscillations on a new class of Delta vehicles, involving an extended-long-tank Delta with an RS-27 engine. The culmination of that portion of the study reported herein has been a successful demonstration of suppression capability on a prior class of vehicle, namely, the long-tank Delta with an MB-3 engine. The demonstration was achieved on the ITOS-F vehicle, and the means of suppression was a resistive lox accumulator. The purpose of this report is to describe the studies which resulted in the successful pogo suppression on the ITOS-F flight.

The current Delta family of vehicles was preceded by the Thor/Agena and Thor/Delta families. Figure 1 depicts this greater class of vehicles in terms of the three sizes of the first stage: short-tank, long-tank, and extended-long-tank configurations. All vehicle configurations, beginning with the inception of Thor/Agena flights in late 1960, have exhibited a major pogo instability during the twenty seconds prior to first-stage main-engine cutoff (MECO). Long-tank and extended-long-tank Delta vehicles have also exhibited two earlier periods of pogo activity.

The term "pogo" is a nickname given to self-excited vibrations experienced by liquid rocket vehicles arising from interactions of the vehicle structure with the propulsion system (Refs. 1 and 2); various studies of the

---

[1] "Prevention of Coupled-Structure - Propulsion Instability," NASA Space Vehicle Design Criteria (Structures), NASA SP-8055, October 1970.

[2] "Final Technical Report, Thor Block 2 Test Program (20 cps Oscillation Problem)," R-3128, North American Aviation, Inc., August 1961.

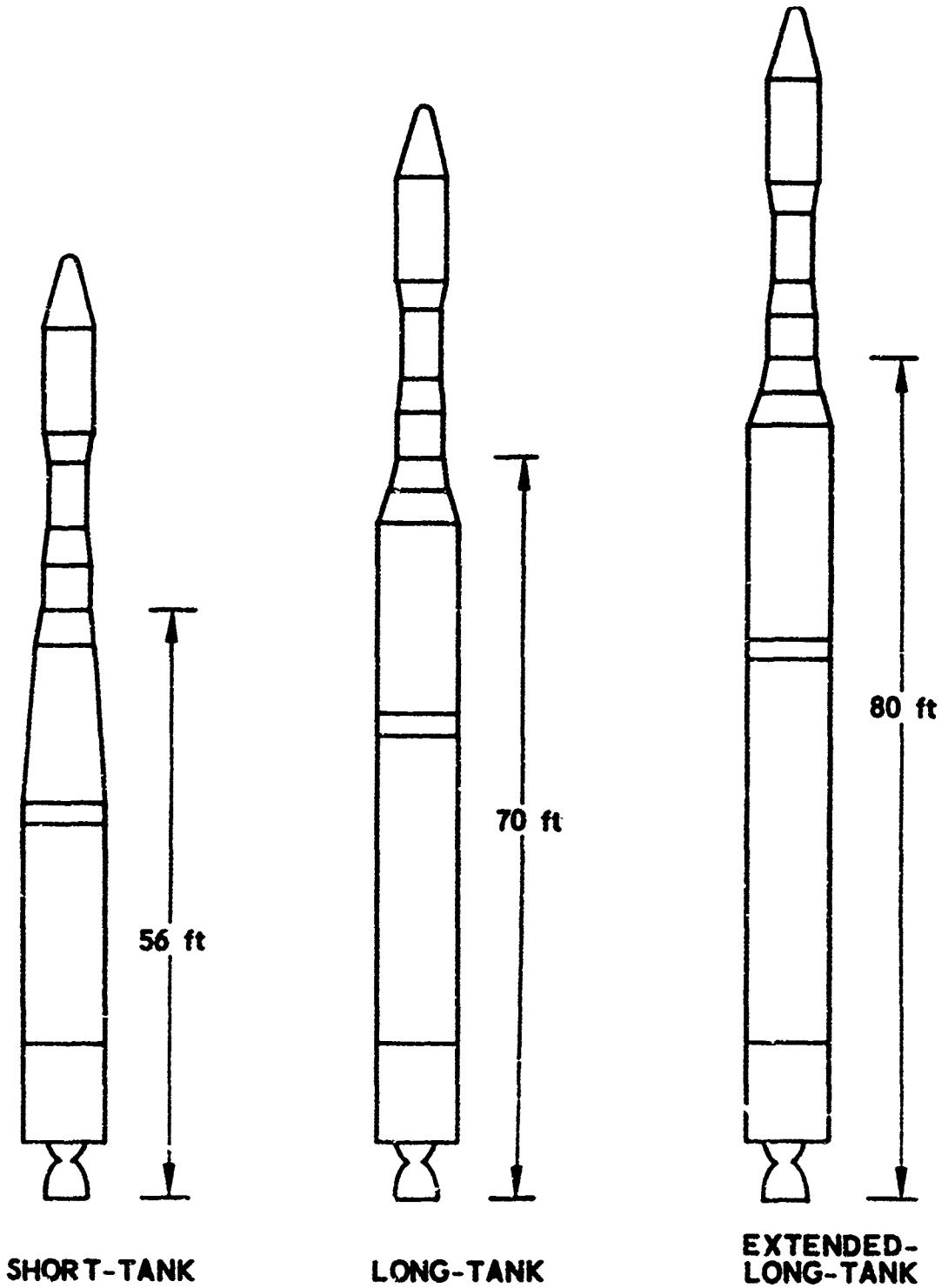

Fig. 1. The Delta Family

phenomenon are reported in Refs. 3 through 8. Figure 2 depicts the pogo events for selected vehicles from each class of Delta vehicle in terms of the variation of longitudinal acceleration amplitude at the first-stage engine gimbal block. The ITOS-F results should be compared to typical results for two earlier vehicles in its class (long-tank Delta with an MB-3 engine): (1) the IDCSP/A having no lox accumulator, and (2) the TD-1 having a lox accumulator but without added flow resistance at the entrance to the accumulator as on the ITOS-F. The reduction in the severity of all three pogo events, most dramatically the MECO event, is evident.

From mid-1963 to mid-1964, a panel of personnel from MDAC, Rocketdyne, Lockheed Missile and Space Company, and The Aerospace Corporation ("Thor 20-CPS Panel") provided a formal mechanism for communication regarding the MECO pogo instability on the short-tank Thor/Agena vehicles.

---

[3] Radovcich, N.A., "Analytical Model for Missile Axial Oscillation Induced by Engine-Structure Coupling," A658522, Lockheed Missiles and Space Company, March 1965.

[4] Davis, W.F., T.F. Lynch, and T.R. Murray, "Thor 20 Cycle Longitudinal Oscillation Study," The Shock and Vibration Bulletin, 34(2), pp. 177-196, December 1964.

[5] Woodward, G.B., and D.H. Gunderson, "Evaluation of High Compliance Device to Suppress 20 cps Longitudinal Oscillations in the Thor Vehicle," TER-65-2, North American Aviation, Inc., July 1965.

[6] Davis, W.F., et al, "Fe sibility Study of Compliant Devices to Eliminate Longitudinal Instability," SM-49005, Douglas Aircraft Company, August 1965.

[7] "Summary Report, Development of a Longitudinal Oscillation Model for the Thor MB-3 Propulsion System," R-6337, North American Aviation, Inc., October 1965.

[8] Lewis, W., "Simplified Analytical Model for Use in Design of Pump-Inlet Accumulators for the Prevention of Liquid-Rocket Longitudinal Oscillation (POGO)," NASA TN D-5394, 1969.

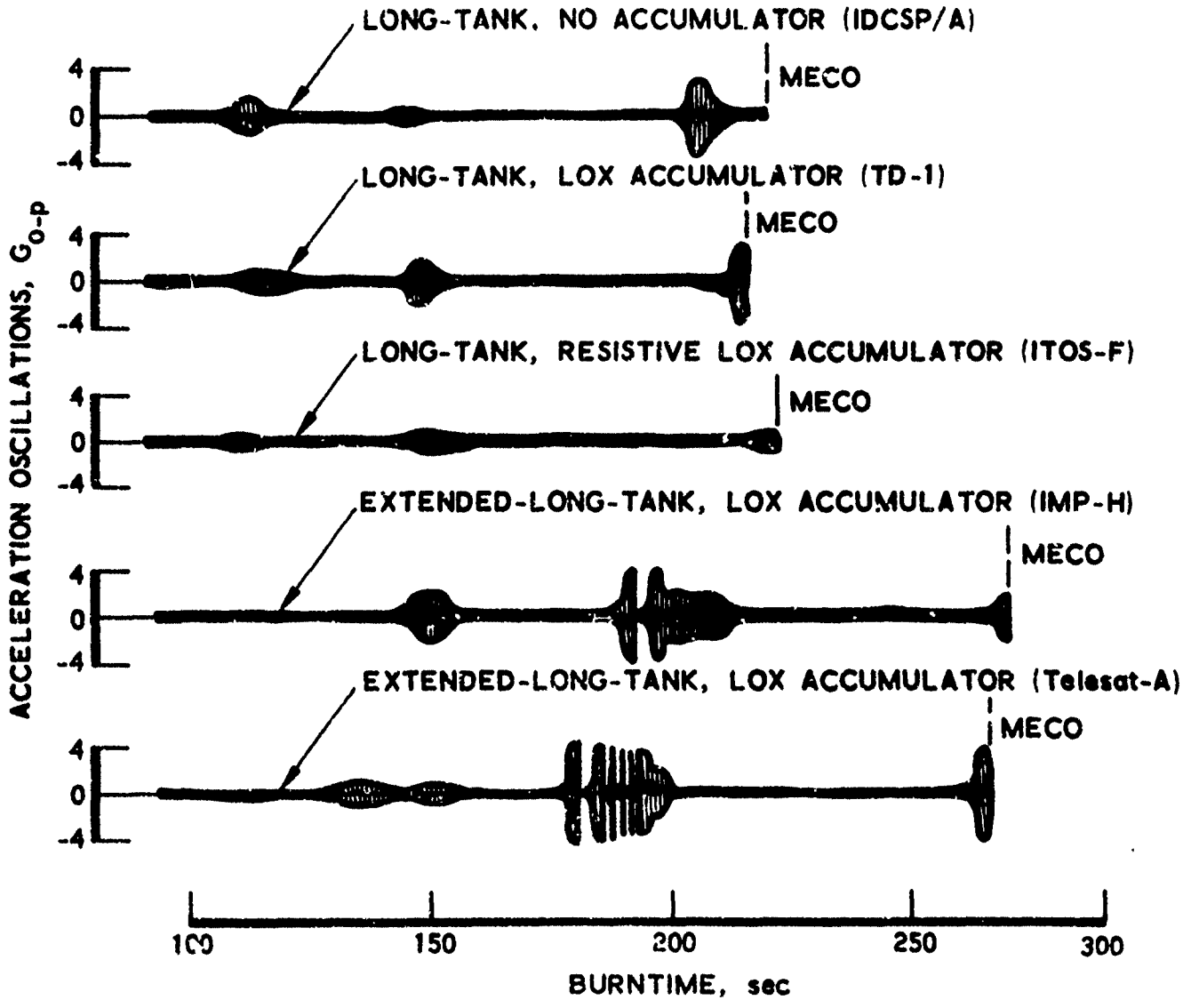

Fig. 2. Gimbal-Block Oscillations for Selected Delta Vehicles

In particular, Aerospace disseminated information obtained from the Titan/Gemini vehicle which was the first demonstration of successful pogo suppression (Ref. 1). In large measure, the success on Titan/Gemini was attributable to a ground test program of the propulsion system which led to its satisfactory mathematical modeling (Ref. 9). Unfortunately, no such test program had been conducted for the Thor propulsion system. Over the years extensive data provided statistical measures of the pogo structural loads. These loads were accommodated by redesign of the aft structure of the Agena, by requalification of Agena equipments to higher sinusoidal vibration levels, and by design of payloads to withstand the loads. A program requirement to suppress the instability did not exist and so studies were terminated. Subsequent success with an accumulator on the Titan IIIB program (Ref. 1) prompted studies of similar devices for the short-tank Thor/Agena (Refs. 5 and 6). It was concluded that stability could be attained. Without a program requirement. vehicle modification was not implemented.

Beginning in 1966, long-tank vehicles replaced the short-tank ones. On long-tank Thor/Delta vehicles two earlier pogo events were first observed (as typified by the IDCPA/A vehicle shown on Fig. 2). Again, statistics were compiled and no action was taken to correct the vehicle. In 1970 MDAC, studying the pogo stability of the extended-long-tank Delta vehicle, predicted higher pogo acceleration levels at MECO than those occurring on the long-tank vehicles. It was evident that some type of corrective device was required, and it was concluded that a slightly modified version of the device employed on the S-II Stage of the Saturn V installed in the lox suction line would stabilize the vehicle. Aerospace, requested to express an opinion, concurred that a lox accumulator would probably result in a stable vehicle at MECO based on the close parallel of the structure/propulsion dynamic characteristics (as then understood) of the Delta vehicle to those of the Titan IIIB vehicle which has been successfully stabilized; no comment could be made for the two earlier pogo events for which no parallel existed on Titan.

---

[9] Wagner, R. G., "Titan II Engine Transfer Function Test Results," Report No. TOR-0059(6471)-9, The Aerospace Corporation, January 1971.

The MDAC recommendation to install the modified Saturn accumulator on extended-long-tank Delta vehicles was accepted. In order to demonstrate feasibility of the concept, an accumulator was flown on a series of long-tank vehicles. The flight data from these long-tank vehicles (as typified in Fig. 2 by the TD-1 results relative to those from IDCSP/A) showed not a stable vehicle as predicted, but a shift to a later time of the MECO instability and the continued presence of the so-called pre-MECO instabilities.

After several flights with the lox accumulator, Aerospace was funded by NASA/Goddard to conduct a parallel study with MDAC. This report summarizes the Aerospace effort in improving the understanding of pogo stability of Delta vehicles with the MB-3 engine. This improved insight led to a modification of the lox accumulator which was responsible for reduced oscillations observed during the ITOS-F flight. The studies reported herein have been carefully coordinated with similar efforts at MDAC. Additional studies are underway for the extended-long-tank vehicle with the new RS-27 engine, but these are too preliminary to be reported at this time.

In the absence of tests to determine propulsion-system characteristics, the approach has been to rely on a thorough analysis of flight data in an attempt to identify the defects in the mathematical model (Ref. 1). In addition to oscillograph traces to spot onset and cessation of periods of instability, power and cross-spectral analyses are employed to yield frequency content as well as relative amplitude and phase relationships between various pressures and accelerations. The periods of instability are related to the eigenvalues from closed-loop stability analyses, a positive real part of a complex eigenvalue indicating an unstable system. Likewise, the relative amplitudes and phases among various flight-measured parameters are directly comparable to the eigenvectors of the closed-loop system. Correction of the stability model is based on improvement of such correlations by changing the equations or the input data or both. Section II discusses the changes made based both on flight data reduction and on theoretical modeling refinements.

Sections III and IV discuss the changes in stability predictions and amplitude-phase relationships which have occurred during the study. The result was a good understanding of the MECO pogo event, while the correlation for the two pre-MECO events, although improved, leaves them still clouded. It was judged possible to modify the accumulator to suppress the MECO instability, without deleterious effect on the pre-MECO instabilities. The ITOS-F flight displayed success with a substantial reduction in the MECO oscillations, as well as an apparent reduction of the pre-MECO events. Section V discusses the rationale behind the accumulator modification and the ground testing of the accumulator required to validate design parameters. Section VI summarizes the effort to date and recommends future action.

SECTION II

CORRECTION OF MATHEMATICAL MODEL

Initial Aerospace stability analyses of the Delta vehicle were conducted using a set of stability equations developed for the Titan vehicle as described in Refs. 10 and 11. It was recognized that the equations were not completely applicable to the Delta vehicle but nonetheless it was felt that only minor modifications would result in a model which would describe the required phenomena. As the study progressed, comparisons of stability predictions with flight data made it apparent that the form of the model was not wholly adequate, and some extensive modifications were made. Additionally, the data used to compute the coefficients of the equations were continuously updated throughout the study. This process of changing the model and comparing it to the flight experience was carried out in three primary stages.

A. CHANGES TO STABILITY EQUATIONS

The first stage of change to the equations involved a modification to include effects of oscillatory outflow from the propellant tanks. A derivation of the equations describing tank potential outflow and an investigation of the potential significance for stability had been undertaken during investigations of the Space Shuttle vehicle (Ref. 12). This change resulted in new equations for tank-bottom pressure and in changes to the generalized force portion of the structural modal response equation.

---

[10] Rubin, S., "Instability Model of Missile Oscillation Due to Propulsion Feedback," Report No. TOR-269(4126)-28, The Aerospace Corporation, September 1964.

[11] Payne, J. G., "Pogo Stability Analysis Program," Report No. TOR-0172 (2122)-10, The Aerospace Corporation, January 1972.

[12] Rubin, S., R. G. Wagner, and J. G. Payne, "Pogo Suppression on Space Shuttle - Early Studies," NASA CR-2210, March 1973.

The following changes were made during a second stage of change: (1) the fuel feedline portion was revised to include the fluid/structural coupling owing to the area change (below the lox aft bulkhead), (2) the lox accumulator equation was modified to include a vertical inertance term (for partial gas fill), (3) the influence of the elevation change along the discharge line was included, and (4) horizontal sections were incorporated in the oxidizer and fuel feedlines ahead of the pumps.

In a third round of change, equations were modified to account for the influence of lateral and rocking pump motions on flow in the feedlines and on generalized forces. Also implemented was a more refined set of combustion relationships (i.e., individual combustion delays of the two propellants).

Appendix A contains a complete description of the current Aerospace pogo stability model. It should also be pointed out that the MDAC stability model has also been upgraded (Ref. 13). The following are among the changes made at the suggestion of Aerospace:

1. Representation of the lox suction line by discrete rather than modal coordinates to account properly for feedline and accumulator resistances
2. Inclusion of discharge elevation change
3. Account for oscillatory tank outflow

B. CHANGES TO INPUT DATA

For initial stability analyses, a complete set of stability-model parameters was obtained from MDAC and used without modification. As the study progressed, all the parameters were examined by both MDAC and Aerospace and few numbers have not been changed. For example, almost all inertance and resistance values have been recomputed. The major changes to the data for the MB-3 engine, however, were for both the lox and fuel pump-inlet cavitation compliances. A recently developed analytical estimation technique

[13] Leuner, T. R. and M. J. Morgan, "MB-3 Powered Long Tank and Extended Long Tank Delta Pogo Stability Analysis," A3-250-ABD3-73-TM-3, McDonnell Douglas Astronautics Company, May 1973.

was employed for both pumps (Ref. 14). It was also possible to infer fuel pump-inlet compliance from flight data. These two developments of compliance are discussed in the next sections.

Figure 3 shows the original and modified values of compliance versus pump cavitation index, with the compliance expressed in terms of a "bubble frequency," f_b, given by

$$f_b = \frac{1}{2\pi}\sqrt{\frac{1}{L_s C_b}}$$

By definition, f_b is the frequency of the system composed of the line inertance, L_s, and the pump compliance, C_b. As explained in Ref. 10, the bubble frequency provides a useful measure of the influence of pump compliance in the hydraulic system.

1. Analytical Estimation of Lox and Fuel Pump-Inlet Compliance

The analytical estimation of lox and fuel compliances was performed by the "stay time" method developed in Ref. 14. The method is based on empirical correlation studies of oxidizer and fuel compliances determined from ground tests of the Rocketdyne H-1, F-1, and J-2 turbopumps. These tests employed sinusoidal perturbations in flow over a range of frequencies. The results for the MB-3 pumps are shown in Fig. 3 by the curves labeled "analytical." Note that they are much lower than the original values employed by MDAC at the higher cavitation indices. In view of these discrepancies, it was decided for Aerospace to undertake an independent review of the flight data from the MB-3 engine.

2. Inference of Fuel Pump-Inlet Compliance from Flight Data

A means of obtaining pump-inlet compliance is to determine one or more propulsion-system resonant frequencies from test data and then infer that value of compliance required in the analytical model to match the observed

[14] Ghahremani, F. G. and S. Rubin, "Empirical Evaluation of Pump Inlet Compliance," Report No. ATR-73(7257)-1, The Aerospace Corporation, August 1972.

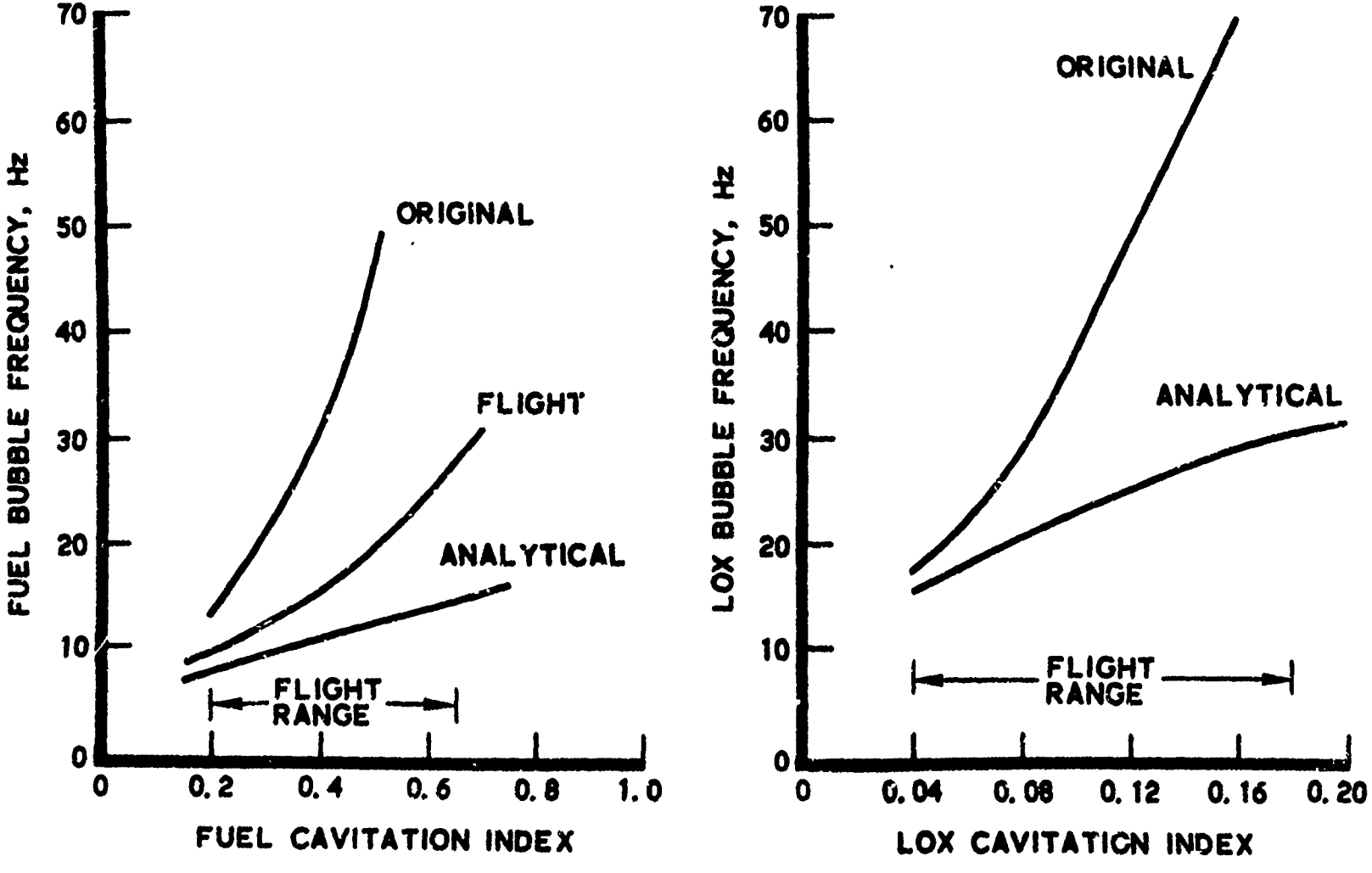

Fig. 3. Bubble Frequencies for Long-Tank Delta Vehicle

frequency or frequencies. Employed is an analytical model including the feedline with an accumulator if present, the line termination impedance provided by the engine, and the unknown pump-inlet compliance. For the short lox line where fluid compressibility is negligible, and when no accumulator is present, it is necessary to determine only the first propulsion-system resonant frequency in order to infer the pump-inlet compliance. With a lox accumulator of known compliance present, both the first and the second resonant frequencies are necessary to deduce the pump-inlet compliance. For the longer fuel feedline, where organ-pipe effects are significant, the first and second resonant frequencies must be identified in order to deduce both the pump-inlet compliance and the effective acoustic speed in the line.

It has generally proven very difficult to identify propulsion-system resonant frequencies from flight data of Delta vehicles. The technique employed (Ref. 1) is to perform power spectral density (PSD) analyses of pump-inlet pressure at a series of flight times and to attempt to identify resonant frequency variation with time to correspond with known variation in cavitation index. PSD's of accelerations must also be obtained in order to identify peaks due to structural resonances so as not to confuse them with peaks due to propulsion resonances.

As reported in Ref. 7, spectral results of pressure and acceleration data were available from the short-tank Thor/Agena Vehicle 344. Concurrent with the study reported herein, MDAC performed PSD calculations on pressure and acceleration data from three long-tank Delta vehicles, OSO-H, HEOS-A2 and TD-1, as well as on data from Telesat-A, an extended-long-tank Delta vehicle. Additionally, MDAC obtained spectrogram displays (Ref. 1) sometimes called "voiceprints", of the data for several of these vehicles.

All of the spectral data mentioned were examined by Aerospace. Attempts to detect the necessary lox resonant frequency information for inference of pump-inlet compliance were unsuccessful. For the fuel

system, only the PSD's from the short-tank Vehicle 344 were judged to indicate the first and second fuel resonant frequencies versus time (Fig. 4). It was this information which served as the basis for our inference of fuel pump-inlet compliance. Some comments should be made regarding the Aerospace interpretation of this Vehicle 344 data. The first fuel system resonant frequency was inferred from peaks in pressure not correlatable with peaks in structural acceleration. On the other hand, the second resonant frequency is based on sporadically visible peaks in the fuel suction pressure spectra which are almost entirely matched by peaks in corresponding acceleration spectra. Our interpretation is that such peaks are only visible in fuel pressure spectra when a structural resonance happens to be coincident such that the fuel mode responds to a greater degree. The confidence with which these peaks can be identified varies with flight time and so the influence of the time varying cavitation index is used to aid in identifying the expected trend in frequencies with time.

Also shown in Fig. 4 is the Rocketdyne first fuel suction system frequency versus flight time as given in Ref. 7. It is our conclusion that the curve from Ref. 7 tracks the first structural mode and was misinterpreted as the fuel-system frequency. Additionally, early use of this data did not account for the influence on the observed frequency of the impedance of the engine termination.

In order to infer the compliance and fluid compressibility, it was necessary to construct a detailed model of the fuel suction system as it existed on Vehicle 344. Figure 5 shows the form of the model of the suction line and Table I lists the engine parameters used in this detailed model. Pump-inlet compliance and fluid bulk modulus were varied in order to match the two fuel frequencies. The second frequency is highly dependent on bulk modulus and a modulus value (B) of 0.43×10^5 lb/in.^{2} produced the best match. An implication of using this value of modulus, which is well below published values, is that the second fuel resonance for the long-tank vehicle

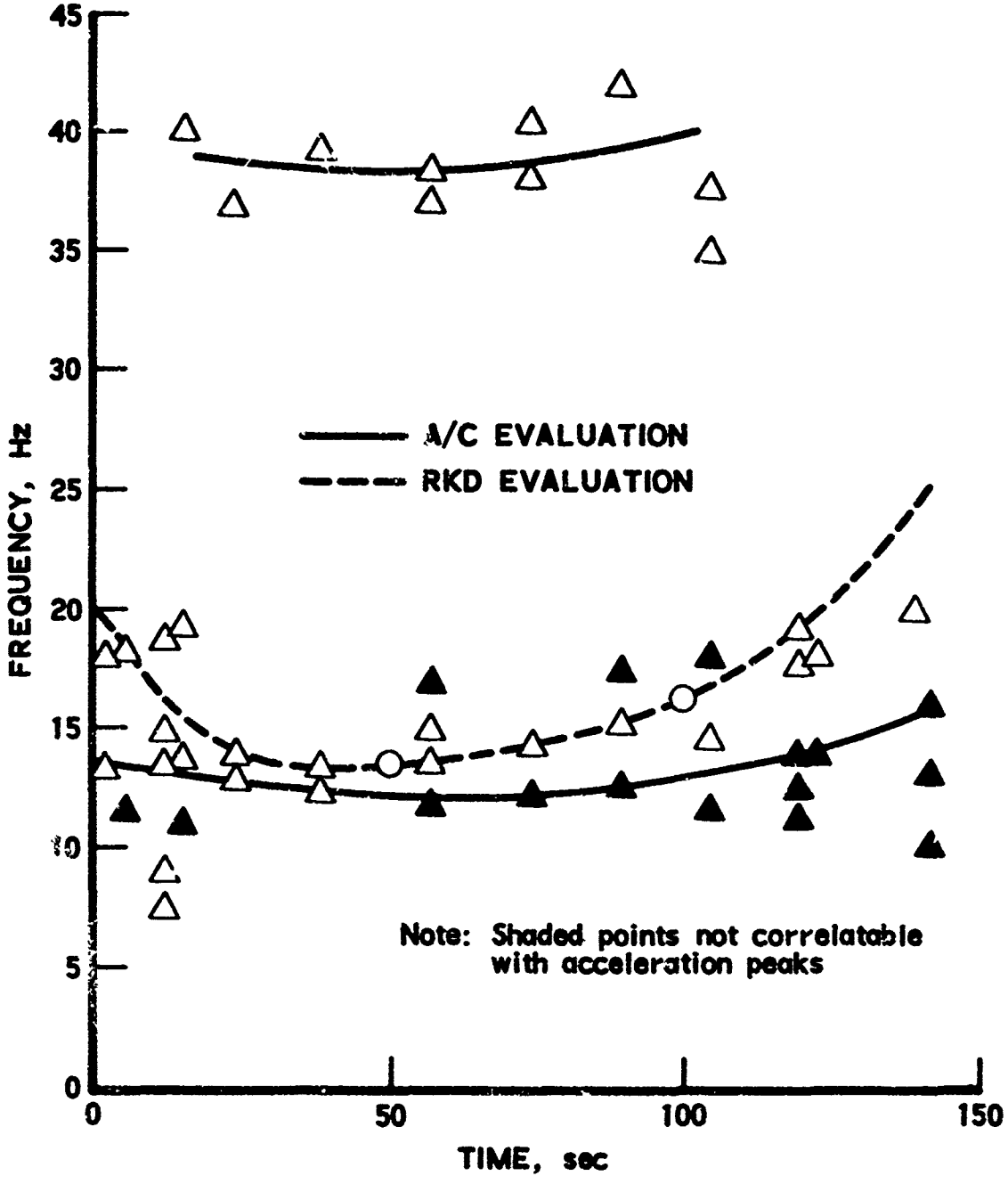

Fig. 4. Vehicle 344 Fuel Suction Pressure Peaks

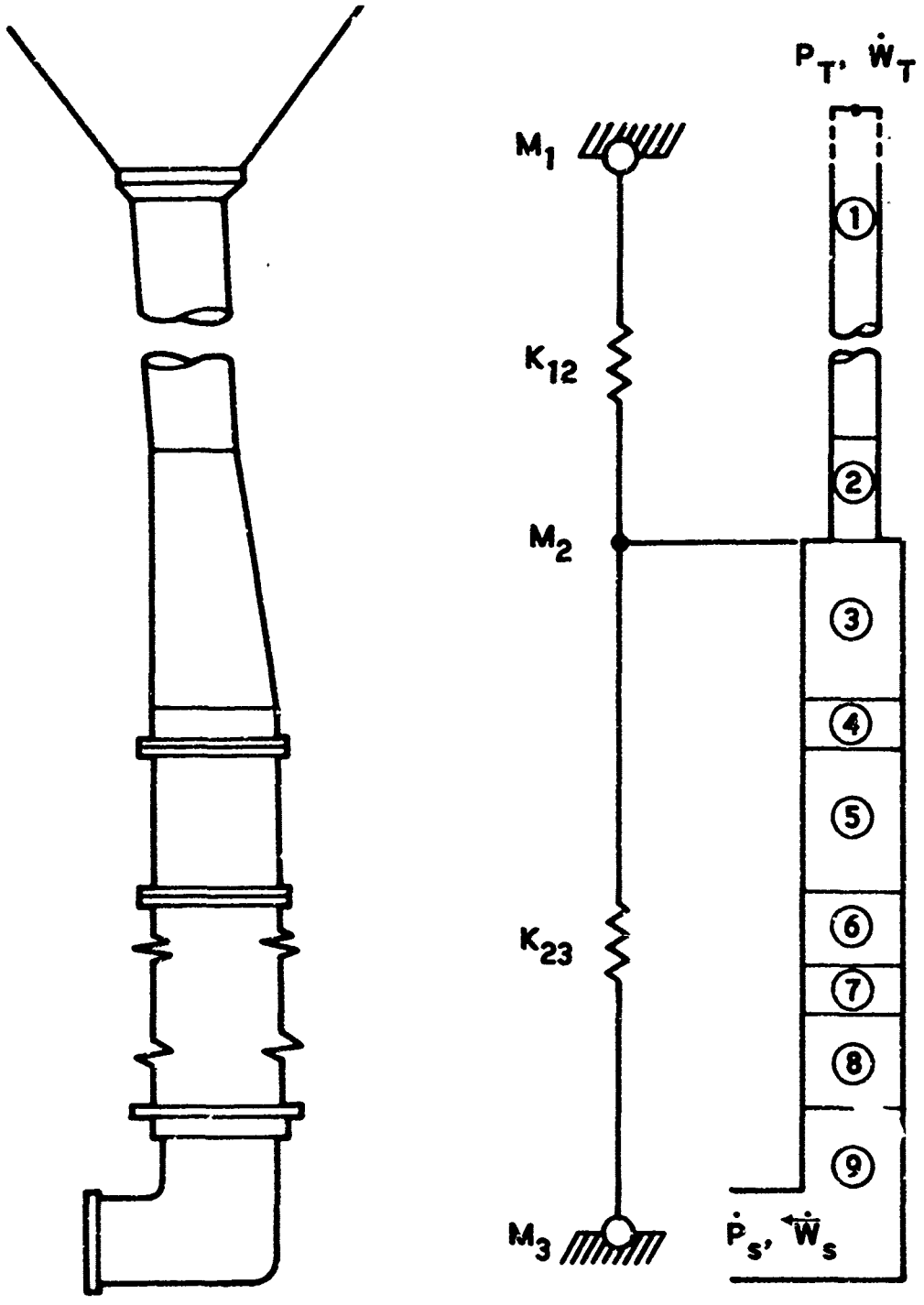

Fig. 5. Delta Fuel Feedline Model Used in Inference of Pump Inlet Compliance and Fluid Compressibility

is then in the 30-Hz region and can play a significant role in pre-MECO stability. MDAC has chosen to base their fuel model on a value of modulus within the range of published values, resulting in a second fuel resonance nearer to 40 Hz.

Table I. Engine System Parameters Used in Inference of Pump-Inlet Compliance and Fluid Compressibility from Vehicle 344

Combustion resistance	=	0.9 sec/in.^{2}
Pump resistance	=	1.17 sec/in.^{2}
Discharge resistance	=	3.06 sec/in.^{2}
Discharge inertance	=	0.0458 sec/in.^{2}
Combustion time lag	=	0.0027 sec
Pump gain	=	2.0

SECTION III

STABILITY PREDICTIONS

As mentioned previously, initial Aerospace stability predictions used the basic Titan stability model and MDAC data. The resulting stability predictions together with the MDAC results current at that time are presented in Figs. 6 and 7. It can be seen that the initial Aerospace results substantiated the MDAC prediction that inclusion of the lox accumulator would stabilize the vehicle near MECO. At pre-MECO times, the two models are not in agreement with each other or with flight experience. The flight data indicates two pre-MECO periods of instability both with and without an accumulator (Fig. 2). The MDAC model at this time predicted one instability with no accumulator and one period of minimum margin with accumulator. The Aerospace model predicted no instabilities, two periods of minimum margin with no accumulator, and a single minimum-margin period with an accumulator.

Figures 8 and 9 show current stability predictions from both the Aerospace and MDAC models (Ref. 13). Both models now show excellent agreement with flight results near MECO in that the incorporation of a lox accumulator does not stabilize the vehicle but only shifts the instability nearer to MECO. No substantial improvement is evident at pre-MECO times except that the frequency of the period of minimum margin in the MDAC model with an accumulator present, and in the Aerospace model with no accumulator present, is closer to the frequency of the second pre-MECO instability seen in flight. Still, neither model predicts two instabilities, or even two periods of minimum margin, for both a vehicle without and with an accumulator.

A natural question upon comparing Figs. 6 and 7 with Figs. 8 and 9 is, "What changes to either the stability equations and/or the input data have led to the improved correlation?" Since most of the changes were made in

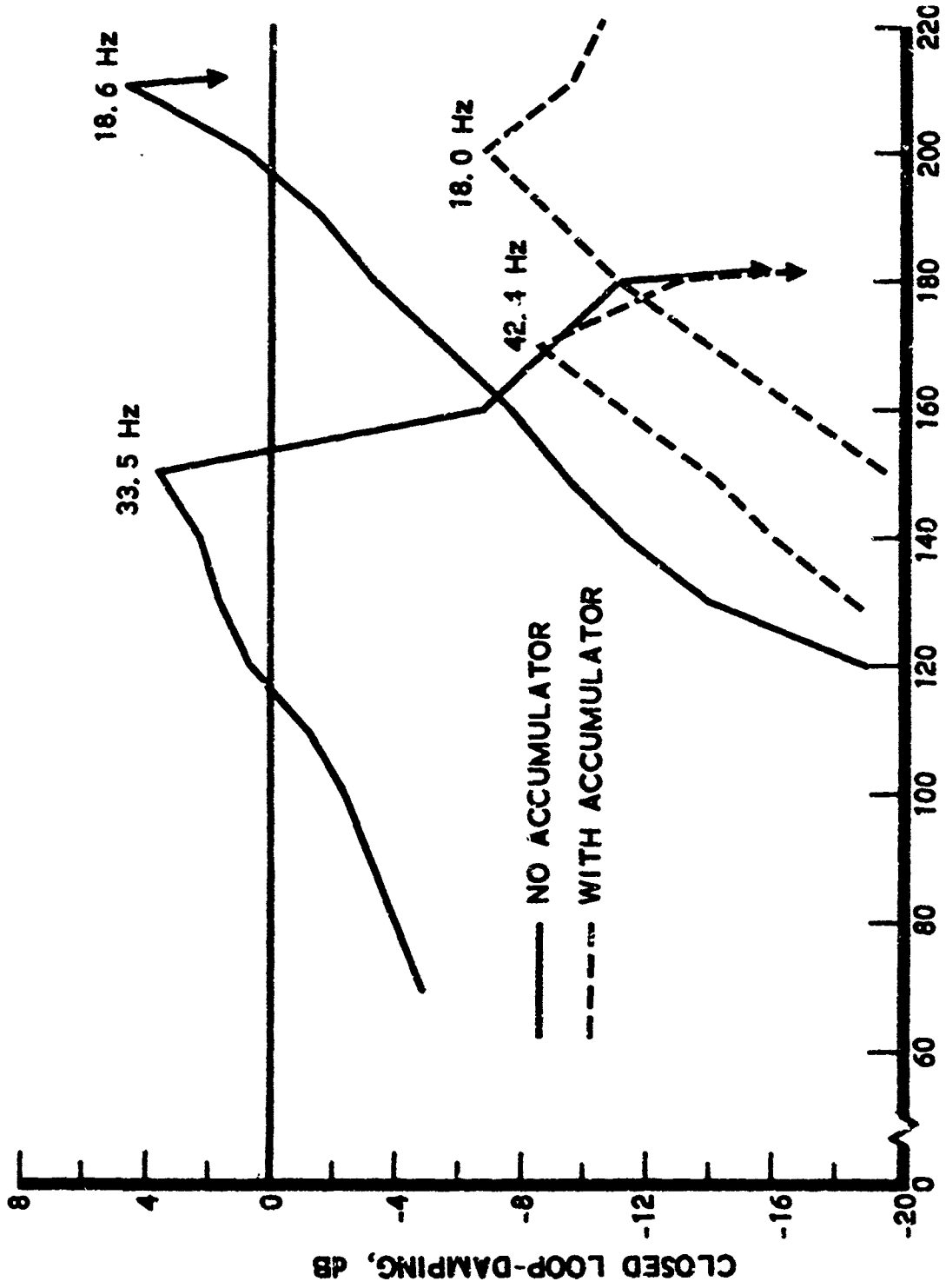

Fig. 6. Initial MDAC Stability Predictions

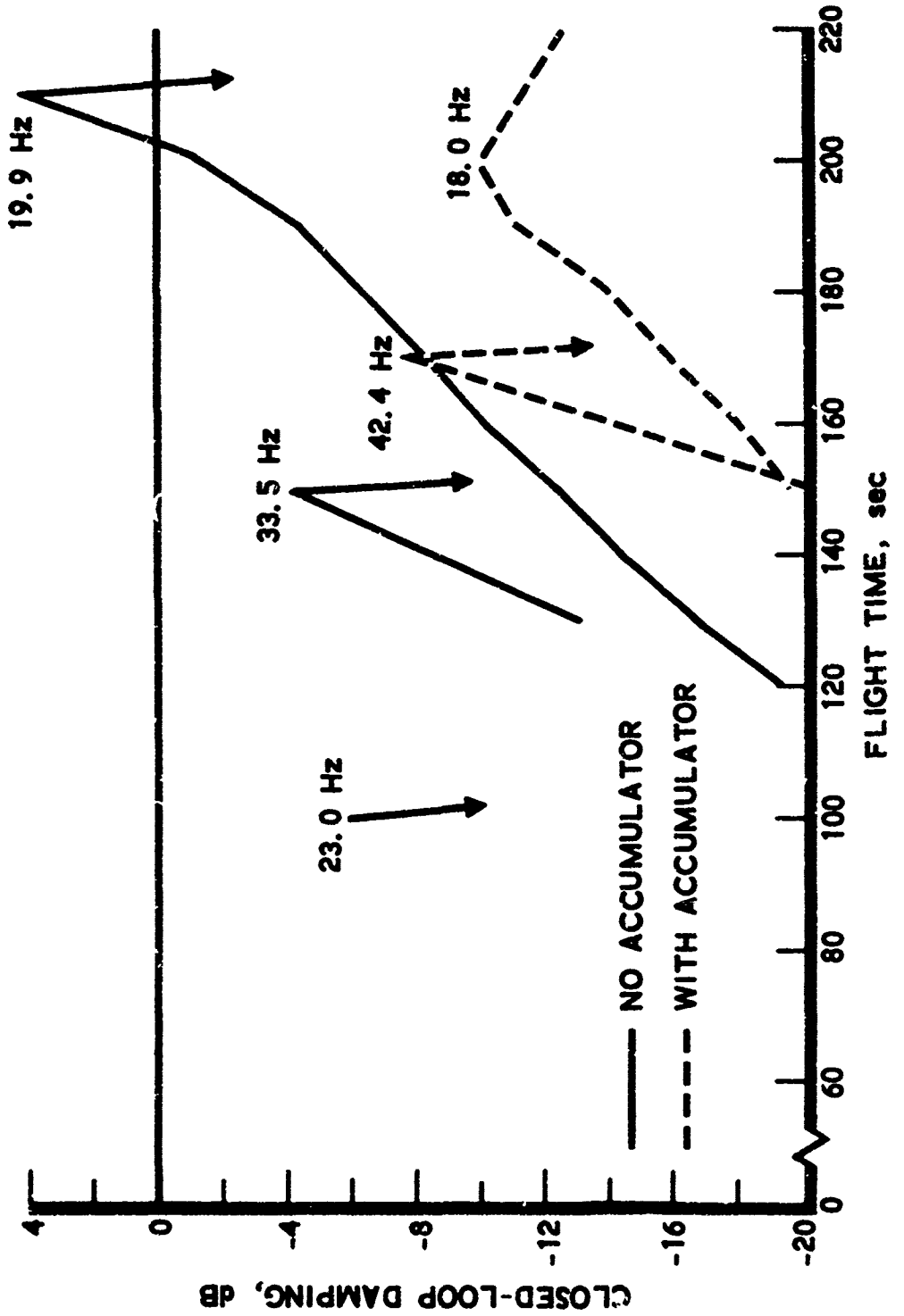

Fig. 7. Initial Aerospace Stability Predictions

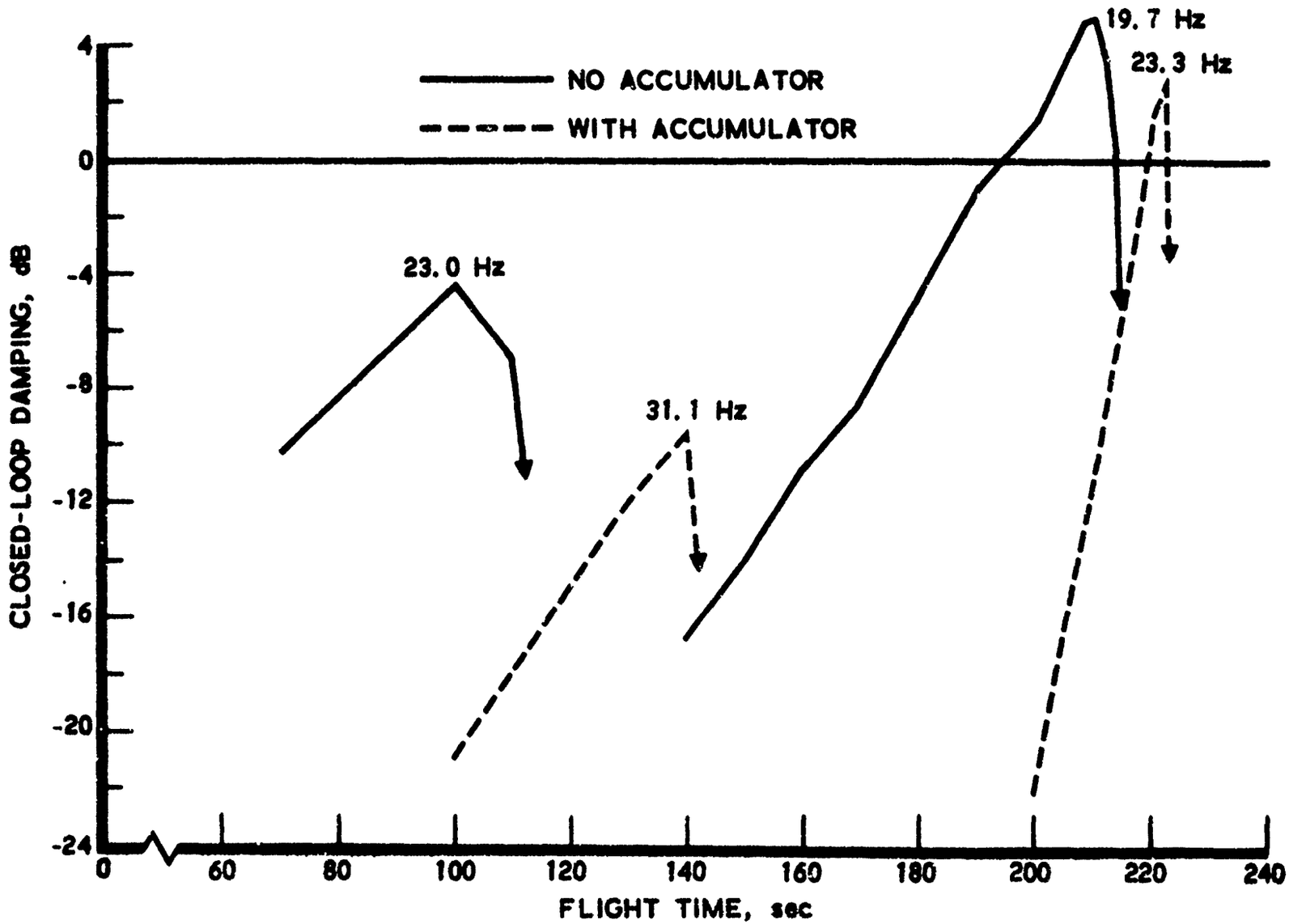

Fig. 8. Current MDAC Stability Predictions

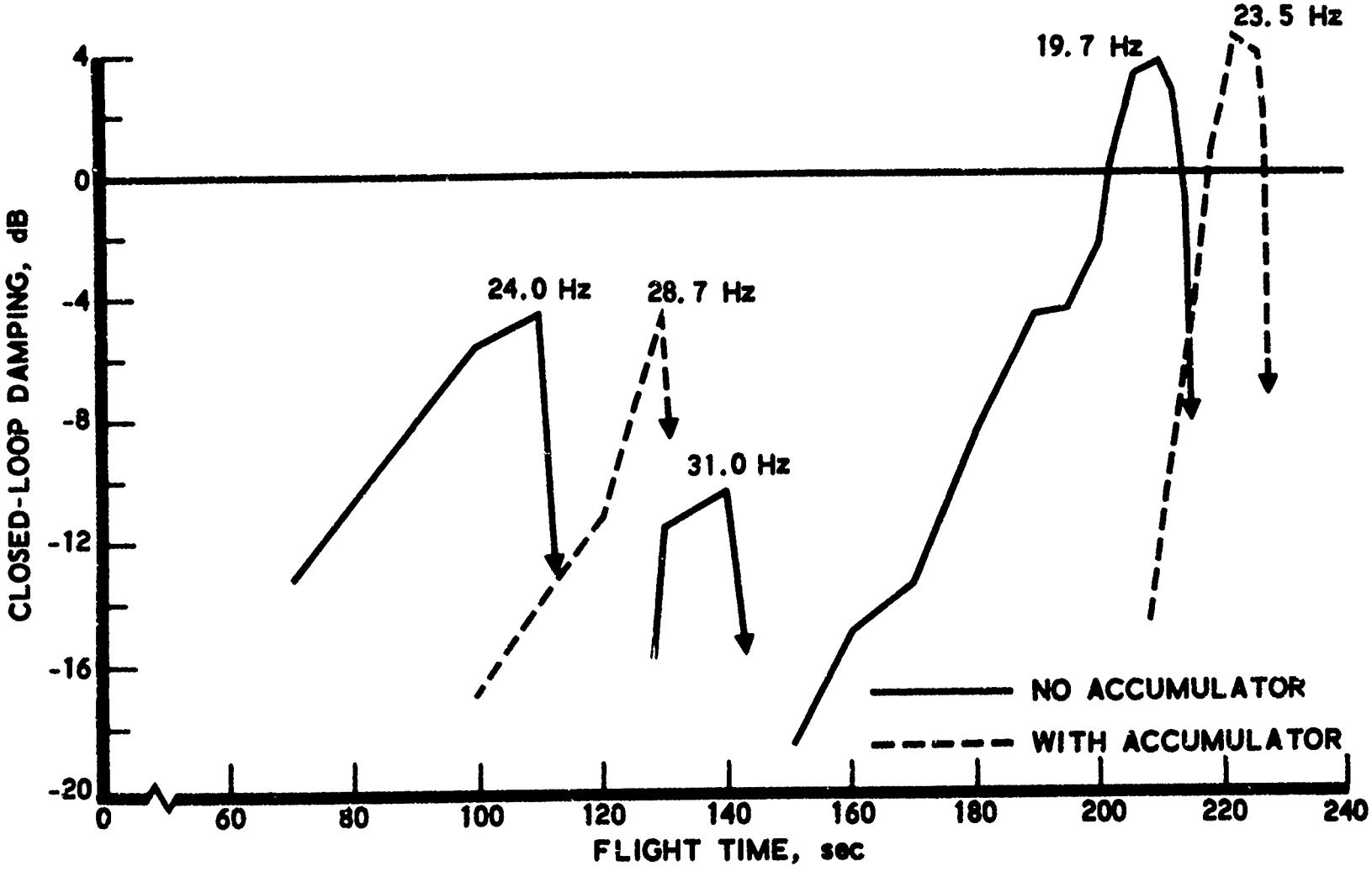

Fig. 9. Current Aerospace Stability Predictions

conjunction with other changes (i.e., the equations and the data were frequently changed together), it is difficult to isolate the influence of individual changes. At MECO, the major influence is the change to the feedline resonant frequencies resulting from changes to pump-inlet compliances and to distributed compliance on the longer fuel line. The resulting second lox line frequency of the configuration with an accumulator is now coincident with the structural frequency near MECO, whereas it was previously not coincident. Any major influence of the fuel system on vehicle stability near MECO has been removed by a substantial lowering of the first fuel frequency.

Although the changes to the stability picture near MECO are explained by the changes to the propulsion-system frequencies, little can be said about the changes earlier in time. Subsequent to the initial analyses, the primary period of interest was MECO; no pre-MECO analyses were conducted following many of the changes. The changes to the propulsion-system frequencies may have a significant influence on pre-MECO results as well as MECO results.

SECTION IV

TRANSFER FUNCTIONS

A method of evaluating accuracy of pogo stability models is comparison of the complex mode shapes (eigenvectors) obtained from the closed-loop stability analysis with amplitude ratio and phase relationships obtained from flight data (Ref. 1). As pointed out in the reference, one of the principle advantages of closed-loop stability analyses vis-a-vis open-loop analyses is the ability to use the resultant mode shapes as a basis of evaluating the stability model. Based on experience with the Titan vehicle, it was felt that this technique would be a useful tool for assessment of the Delta stability model.

Application of the technique requires careful and extensive flight data reduction. Power-spectral densities (PSD), cross-spectral densities (XSD), coherence functions, and transfer functions must be determined for parameters of interest at a sequence of flight times. The transfer functions are the desired amplitude and phase relationships; our experience has led to the criterion that these relationships should be considered invalid when the coherence is less than 0.8. This process can, in general, be simplified for evaluation of the structural modes to only PSD plots of structural accelerations. This simplification is possible because the structural modes are very lightly damped, the coherence among the accelerations is essentially unity, and the relative phasing (0 or 180 deg) is usually known.

For the Delta vehicle, it has generally been possible to obtain valid relationships (coherence ≥ 0.8) only during periods of instability. In contrast, for the Titan vehicle, it has generally been possible to determine the ratios of both suction and chamber pressures to gimbal block acceleration in the first longitudinal mode throughout most of Stage I burn as shown in Fig. 10. It is uncertain whether the character of the system is inherently different or whether different data reduction techniques are responsible. Nonetheless, the transfer function information obtained for the Delta vehicle has been quite useful in evaluating the stability model.

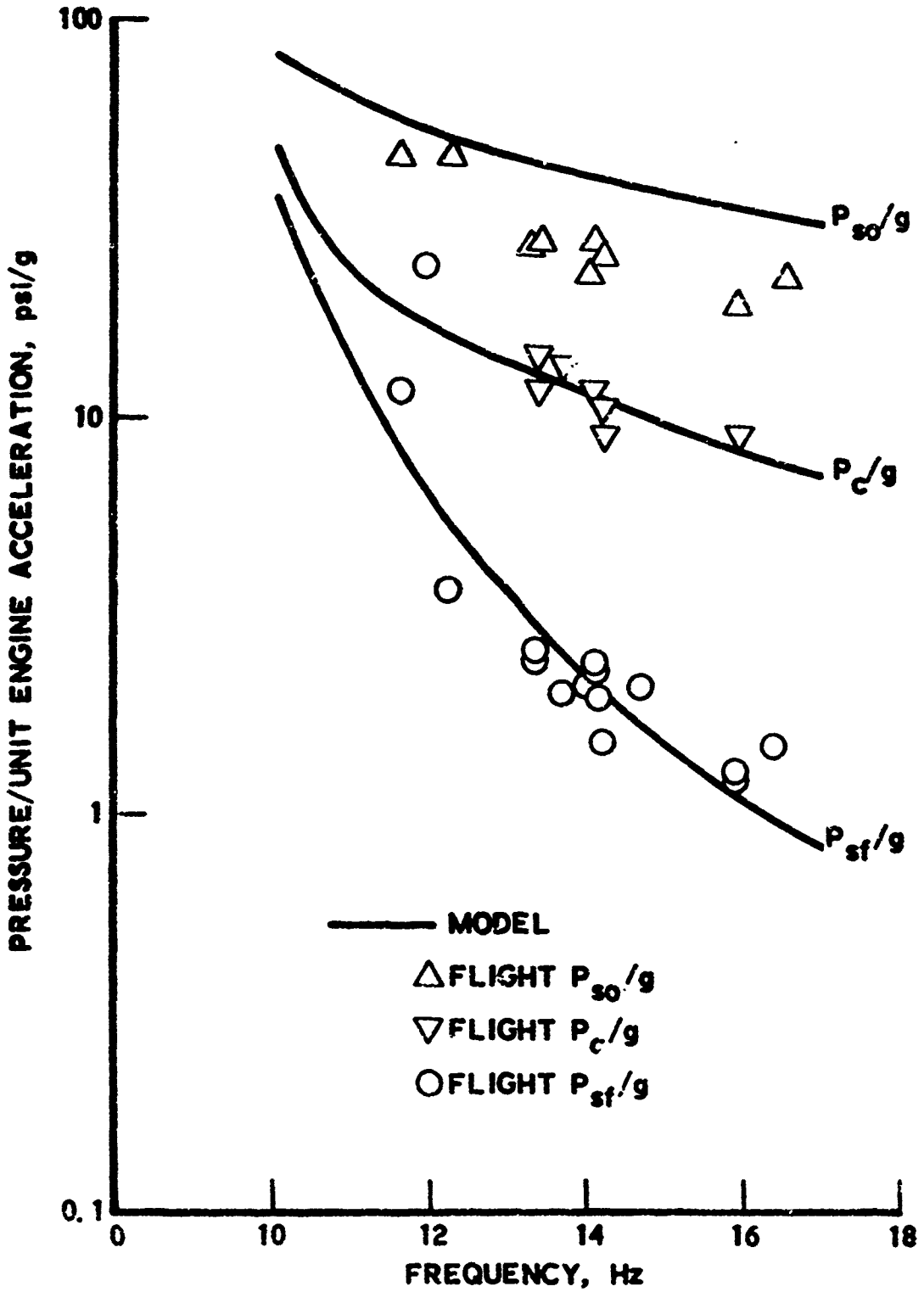

Fig. 10. Suction and Chamber Pressure per Unit Engine Acceleration in the First Longitudinal Mode for the Titan III Vehicle

The earliest model evaluation via transfer functions revealed that the MDAC and Aerospace models were in poor agreement with each other as well as with flight data. Both Aerospace and MDAC made a series of changes to their stability models (the Aerospace changes are described in Section VI). Another change was to correct the lox suction pressure computed in the model to account for the actual location of the flight measurement (above the lox elbow). Following the changes, the two models yielded results in good agreement with each other at MECO.

Relationships of flight data to the Aerospace model at MECO are shown in Figs. 11 and 12. The comparison with flight data is somewhat clouded because of the sparseness of good flight data; e.g., it is difficult to identify consistent trends versus frequency over a wide frequency range as was done for the Titan data. Additionally, obtaining high coherence data only during periods of instability means that nonlinear effects may be present. It is of interest to note that the data from the Telesat flight, which had the most careful data reduction (contiguous, more narrow time slices), produced trends in all the transfer functions which agree with those from the stability models (see especially Fig. 12). The correlation is considered to be moderately good and provides a basis for a reasonable level of confidence in the stability model for the MECO period.

At pre-MECO times the stability model produces transfer functions which are in very poor agreement with the flight data. It must be recalled, however, that the stability predictions during these periods are also not in good agreement; perhaps whatever model changes improve the stability portrait will improve transfer functions.

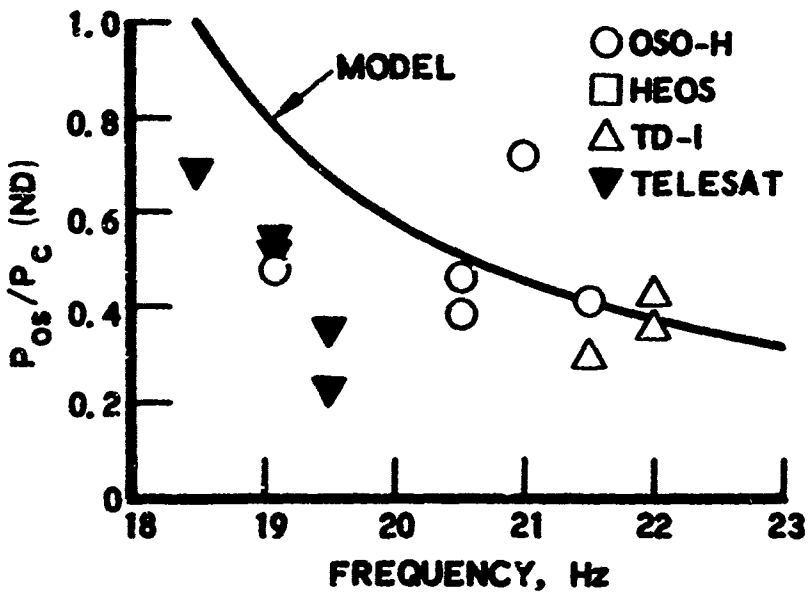

Fig. 11. Lox Suction Pressure per Unit Chamber Pressure for Delta Vehicle at MECO

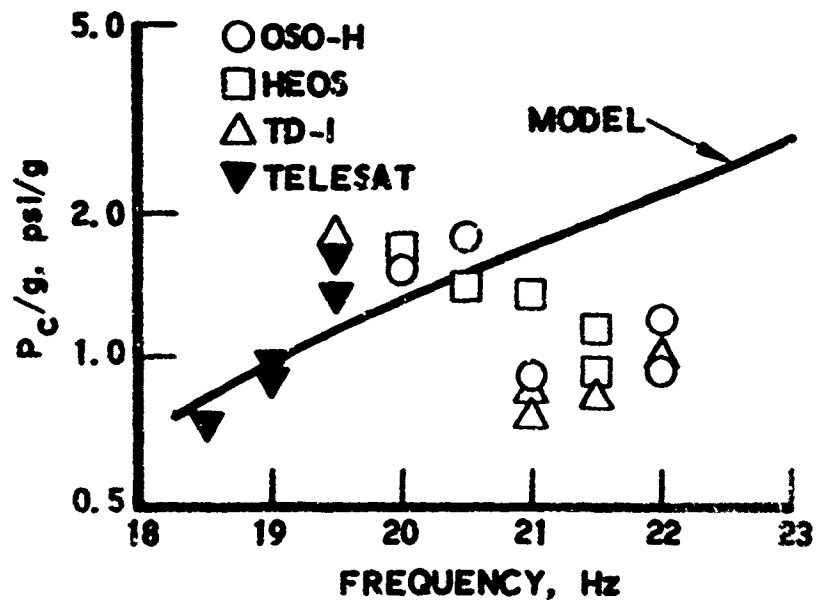

Fig. 12. Chamber Pressure per Unit Engine Acceleration for Delta Vehicle at MECO

SECTION V

MODIFICATIONS TO LOX ACCUMULATOR

A. OPTIMIZATION OF RESISTANCE

Historically, the function of an accumulator has been to detune the propulsion system from the structural system. Prior to the first flight of a Delta vehicle with an accumulator, it was felt that the particular accumulator would accomplish this detuning; an approach successfully demonstrated on the Titan and Saturn vehicles. Unfortunately, this assumption was based on an inadequate model of the lox suction system.

The lox feed system model used at the time did not reveal that incorporation of the accumulator, while detuning the first lox mode from the structure, would introduce a second lox mode that would lead to an instability. Had it been possible to locate the accumulator nearer to the pump inlet, this situation would not have occurred. Since it was judged impractical to relocate the accumulator nearer to the pump, an alternate solution was required. The approach recommended by Aerospace was to add resistance via orifices to the entrance of the existing accumulator. It was hoped that the resulting damping increase to the second feedline mode would be sufficient to eliminate the instability.

A study was undertaken to define an optimum accumulator resistance by studying its effect on the feedline flow impedance looking toward the tank from a position just upstream of the pump cavitation. This impedance, Z_ℓ, can be written in real and imaginary terms

$$Z_\ell = R + iX \tag{1}$$

A maximum value of the real part, R, was the criterion for an optimum accumulator resistance. Referring to Fig. 13, this line impedance can be written

$$Z_\ell = Z_3 + \frac{1}{\frac{1}{Z_1} + \frac{1}{Z_a}}$$

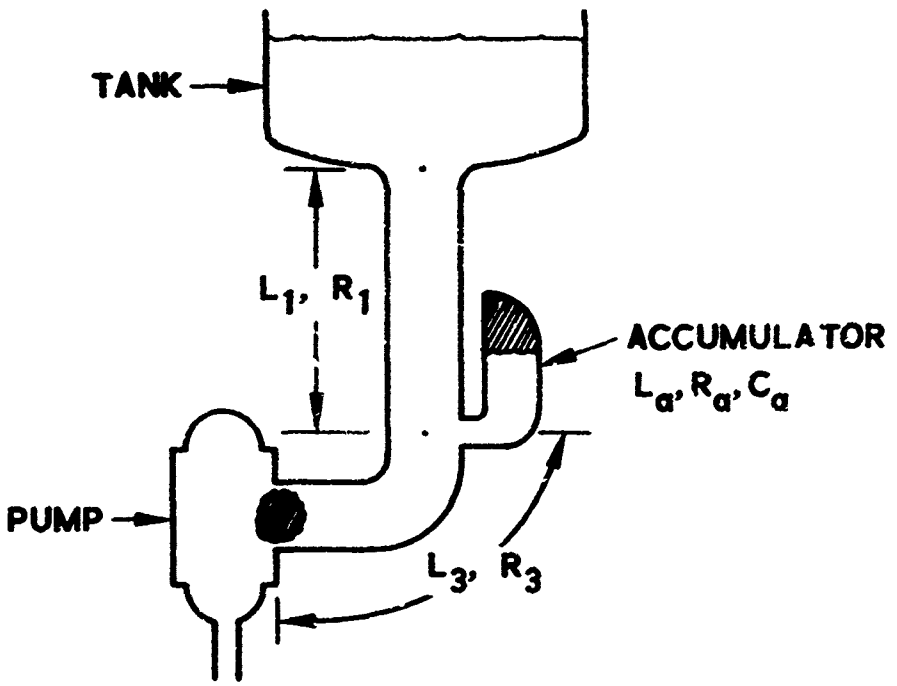

Fig. 13. Schematic of Lox Propulsion System

where $Z_3 = R_3 + i\omega L_3$, $Z_1 = R_1 + i\omega L_1$, and $Z_a = R_a + i\omega L_a$. The accumulator impedance Z_a reflects the fact that the accumulator compliance, C_a, is negligible in the frequency range of interest.

For convenience, the search for an optimum resistance was conducted at a constant frequency of 150 rad/sec (23.9 Hz), a value approximately equal to the line resonant frequency at MECO both with and without an accumulator. A plot of the imaginary part, X, versus the real part, R, of the line impedance as a function of the accumulator resistance, R_a, is shown below in Fig. 14. Curves are shown for two values of the accumulator inertance, L_a; the value $L_a = 0.0006$ sec/in.^{2} pertains to the unmodified accumulator. It can be seen that an optimum accumulator resistance does exist (i.e., it produces a maximum of R), a value of $R_a = 0.32$ sec/in.^{2} being optimum for $L_a = 0.0006$ sec^2/in.^{2}. The effect of accumulator inertance, L_a, can also be seen; a doubling of L_a significantly lowers the maximum value of R but produces little changes in the optimum value of R_a. Since a maximum of R is desired, any increase in inertance over the value for the unmodified accumulator should be kept to a minimum.

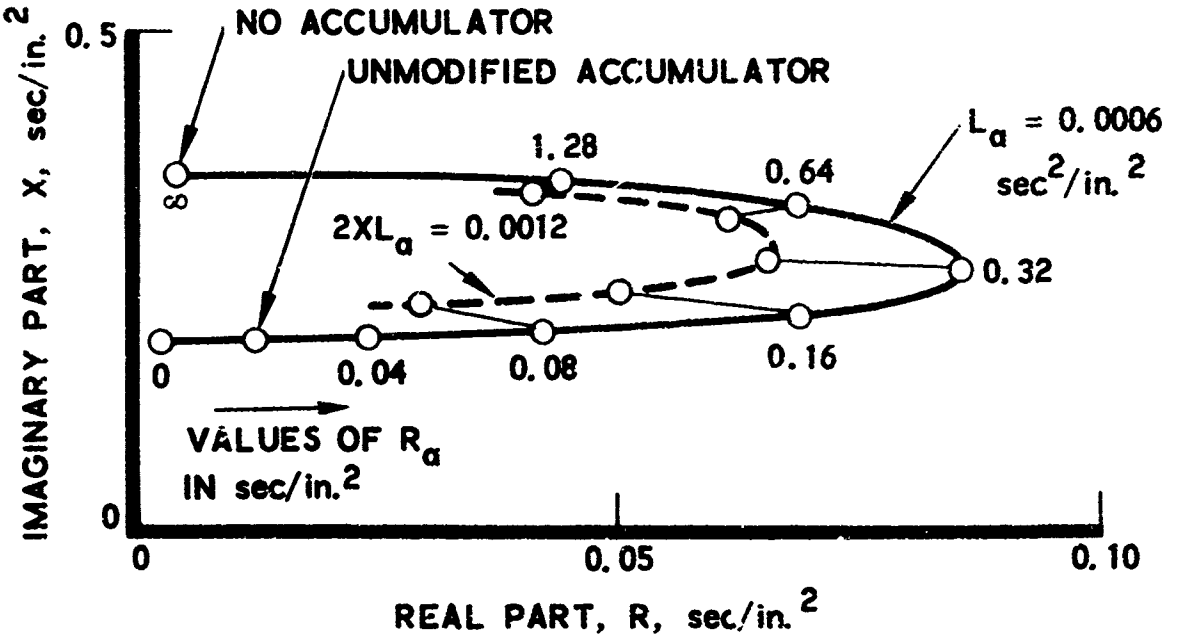

Fig. 14. Effect of Accumulator Resistance on Lox Feedline Impedance

That the optimum R_a as defined by the feedline impedance would also be an optimum in terms of vehicle stability was verified by performing stability analyses versus flight time for selected resistance values. Since the modifications studied were expected to increase accumulator inertance somewhat, L_a was chosen as 0.001 sec^2/in.^{2} for this study. The results are shown in Figs. 15 and 16. These figures show that near optimum resistance will produce a major improvement in stability margin, while there is no value of added resistance which will produce a gain greater than one of the two configurations previously flown (i.e., no accumulator or unmodified accumulator). Further, the optimum obtained via stability analyses agrees very closely with that obtained via the feedline impedance procedure.

B. DEFINITION OF RESISTANCE

The results of the previous section show that it is possible to achieve an optimum vehicle stability condition if the accumulator can be modified so

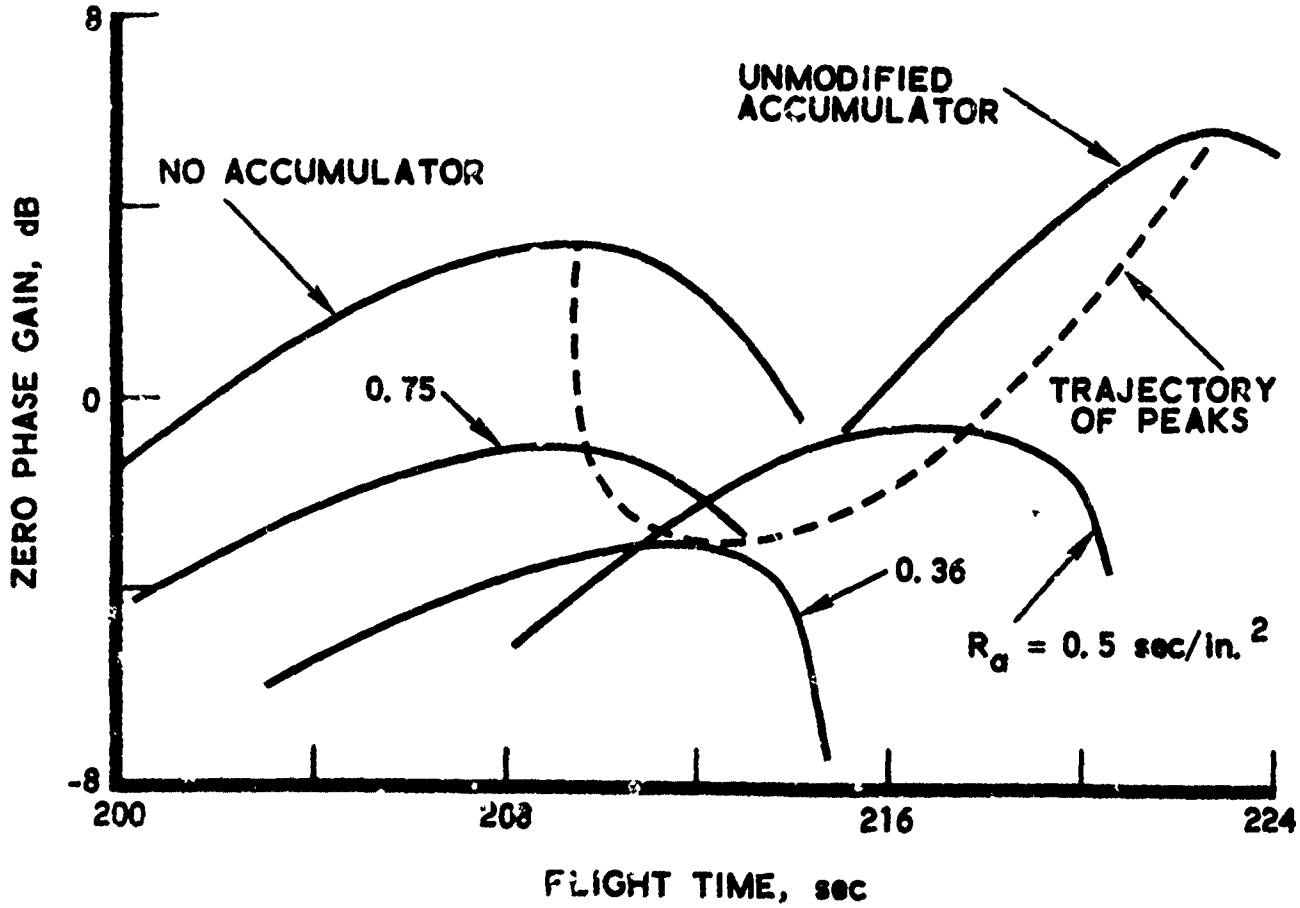

Fig. 15. MECO Stability as a Function of Accumulator Resistance

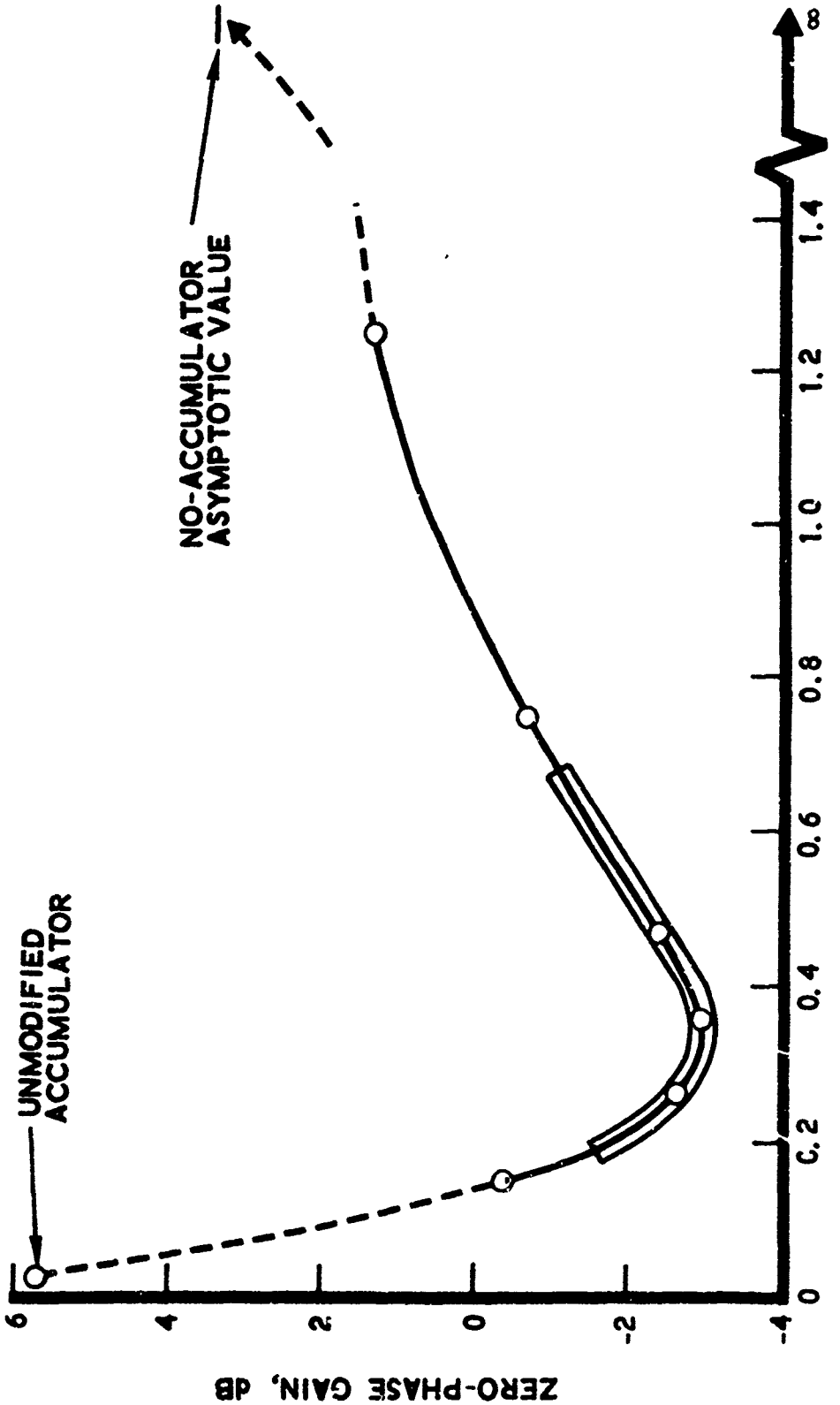

Fig. 16. Influence of Accumulator Resistance on MECO Stability

as to produce a certain resistance. Unfortunately, the prediction of resistance due to purely oscillatory flow as a function of fluid properties and flow-passage geometry is not a well-defined procedure.

In order to minimize inertance, it was proposed to modify the accumulator by placing a thin orifice plate containing a series of small holes within the entrance region to the accumulator. The final configuration containing this so-called "hatband" is shown in Fig. 17. The accumulator modification for the ITOS-E flight did not have the benefit of a ground testing program to confirm that the desired resistance was achieved. This decision was based on scheduling constraints and was rationalized with the fact that (1) previous ITOS missions had flown both with and without an accumulator and had experienced about the same pogo levels, and (2) that any added accumulator resistance is helpful in theory (Fig. 15).

Two sources of data for estimating resistance were known to Aerospace prior to ITOS-E flight. The first source was frequency-response tests of the fuel bladder-type accumulator now flying on the Titan vehicle (Ref. 15), and the second source was acoustic tests above 1 kHz directed toward suppressing combustion instability (Ref. 16). Both tests involved oscillatory flow through various patterns of holes similar to the conditions of the proposed modified accumulator.

The two sources of data seemed to yield contradictory results. In interpreting the Titan data, it was assumed that a major portion of the total resistance was due to orifice sistance as opposed to bladder deformation or rubbing. It was further assumed that the RA product, where A is the total open area of the pattern of holes, should be a constant. With this interpretation of the Titan data, and allowing for scatter and uncertainty in the data, a range of $0.1 \leq R_a A \leq 0.32$ was derived.

---

[15] Zehnle, R., "T-III-M Phase 1A Frequency Response Test - Fuel Accumulator," TM 0472/20-2-68, Martin Marietta Corporation, June 1968.

[16] Garrison, G. D., et al, "Suppression of Combustion Oscillations with Mechanical Damping Devices - Interim Report," PWA FR 3299, Pratt and Whitney Aircraft, August 1969.

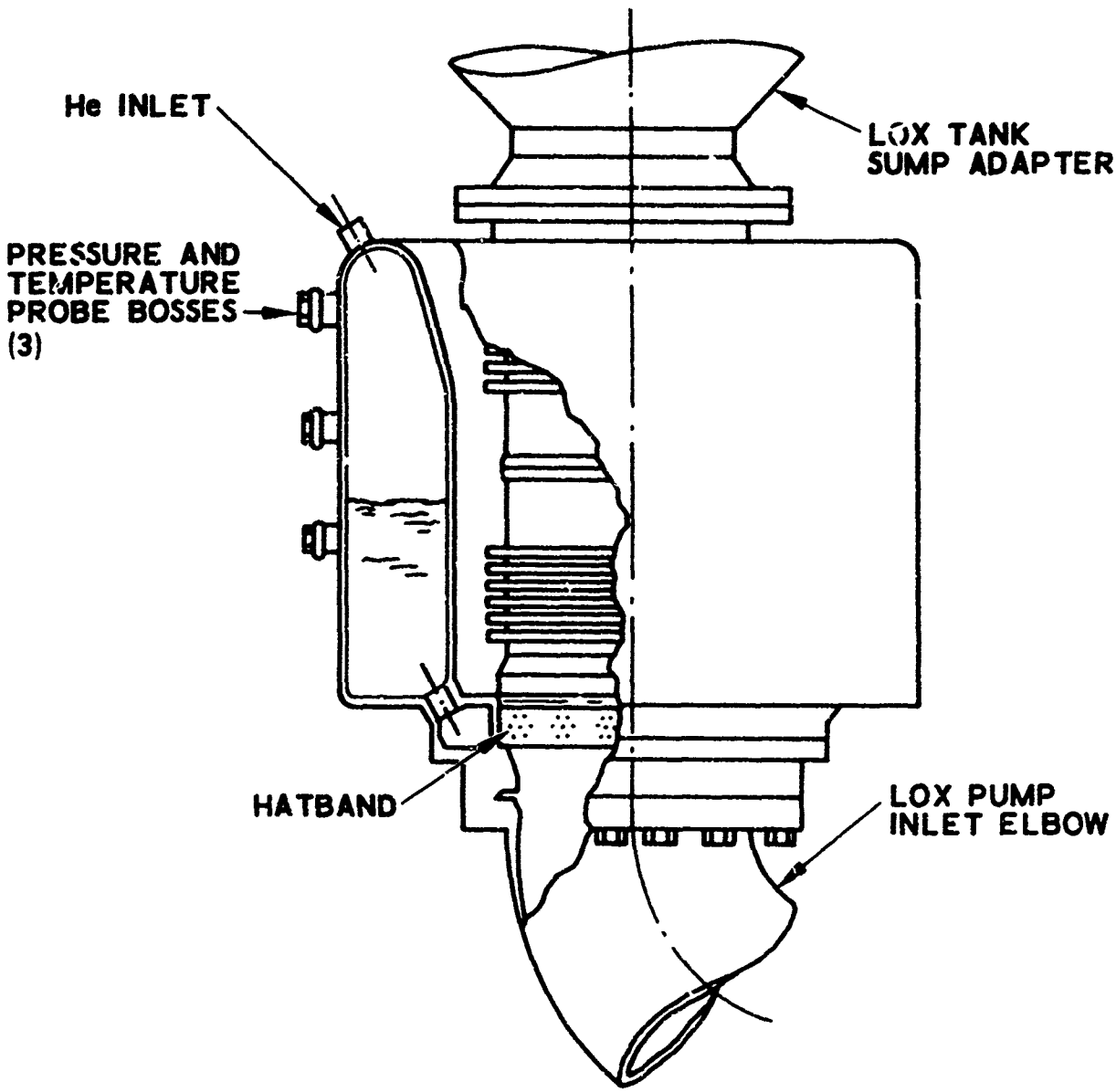

Fig. 17. ITOS-E Lox Accumulator

The Titan data, involving liquid (Aerozine) flow oscillations in the frequency range of 3 to 30 Hz, showed resistance to be reasonably independent of flow amplitude. However, the acoustic data, based on N_2 gas flow in the 2 to 8 kHz range, showed both a linear and nonlinear region. The linear acoustic data correlated well with Rayleigh drag theory, but when this linear data was used to estimate the Titan test resistance, an orifice resistance an order of magnitude lower than measured on the Titan tests was computed. Since it was felt at the time that orifice effects should have been dominant for the Titan configuration, it was decided to base the design on the experimental Titan data. Examination of Fig. 16 reveals that the choice of an open area of 0.5 $in.^2$ for the hole pattern, resulting in a range of R_a of from 0.2 to 0.64 (corresponding to $0.1 \leq R_a A \leq 0.32$), will be optimum for stability. The configuration for ITOS-E contained a pattern of 1/16-in. diameter holes in a 0.030-in. hatband to yield the desired 0.5-$in.^2$ area.

This configuration was flown on the ITOS-E vehicle and resulted in a stability profile very similar to that of a vehicle with no accumulator, indicating that the resistance obtained with the 0.5-$in.^2$ area was effectively sufficient to block the accumulator. Concurrent with the flight, an additional source of resistance data was pointed out to Aerospace by NASA/Goddard personnel (Refs. 17 and 18). The new data appeared to be superior to the previous data since it was the result of carefully controlled, well-documented experiments with two liquids (allowing the effect of viscosity to be assessed), and it did cover the frequency range of interest for the Delta vehicle. Unlike the Titan data, there were no other potential sources of losses, and there was little scatter in the data.

---

[17] Thurston, G. B., and C. E. Martin, "Periodic Fluid Flow Through Circular Orifices," J. A. S. A., 25(1), January 1953, p. 26.

[18] Thurston, G. B., "Periodic Fluid Flow Through Circular Tubes," J. A. S. A., 24(6), November 1952, p. 653.

The data of Refs. 17 and 18 correlate well with the previously evaluated acoustic data in that both linear and nonlinear regions are present. The linear portions correlate well with Rayleigh theory as did the acoustic data. Additionally, it was discovered that when the resistance per unit area was plotted versus particle velocity, the new data correlate reasonably well with the acoustic data in the nonlinear region. These data, when applied to the ITOS-E accumulator, indicate operation in the nonlinear region for flow amplitudes corresponding to very small vehicle acceleration amplitudes; thus, the accumulator would be effectively blocked during flight. In retrospect, it was concluded that the orifices were not, in fact, the major source of losses for the Titan accumulator as had been previously supposed.

Based on the latest data, it was necessary to define a new hatband configuration for optimum stability. It was decided that a pulsing test of several candidate configurations would be essential; there were still some questions regarding resistance; e.g., the data in Refs. 17 and 18 were collected with single orifices, rather than orifice arrays, and without the superimposed random flow oscillations which characterize the flight situation. Pulsing tests were conducted by MDAC with Aerospace providing a basis for the test plan. It was suggested by Aerospace that testing include not only variations in sinusoidal input levels (designed to evaluate the nonlinear characteristics displayed in Refs. 17 and 18) but also determine the influence of random inputs superimposed on the sinusoids. Hatband configurations having various open areas and several liquids (to assess the influence of viscosity) were used in the tests.

The test data for purely sinusoidal flows correlated well with that of Refs. 17 and 18 at frequencies up to 20 Hz but showed an unexplained higher resistance at higher frequencies. In general, the addition of random inputs had the effect of providing a resistance "floor," as depicted in Fig. 18. One unexpected trend was a slight decrease in resistance with increasing viscosity; the lowest viscosity fluid tested (a Freon) had a viscosity not very

different from that of lox, and the dependence was not a strong one. In summary, it was felt that the resistance was well defined by the tests.

The tests showed that an open area of 1.5 $in.^2$ would produce a resistance very near the optimum value and fairly independent of flow amplitude (Fig. 18) up to that corresponding to a gimbal-block acceleration amplitude of about 1 g. A hatband having this area was incorporated into the ITOS-F vehicle flown on 6 November 1973. Examination of oscillograph traces of filtered gimbal-block acceleration from ITOS-F shows clearly that the levels during the MECO and second pre-MECO pogo events are dramatically reduced relative to levels observed on previous long-tank vehicles, and the level during the first pre-MECO period is unaffected (Fig. 19). Figure 20 shows the envelopes of guidance-compartment accelerations near MECO from five ITOS flights and shows that the 1.5-$in.^2$ resistive accumulator produced levels lower than vehicles with or without an accumulator. (Recall from Section V-B that the 0.5-$in.^2$ resistive accumulator produced a resistance sufficiently high to effectively block the accumulator.)

It cannot be concluded with certainty whether the ITOS-F vehicle was stable at MECO as predicted analytically. However, the character of the data does not indicate the classic build-up and decay generally associated with an instability but appears similar to low-level random response. This change in character was also observed, but to a lesser degree, during the second pre-MECO period.

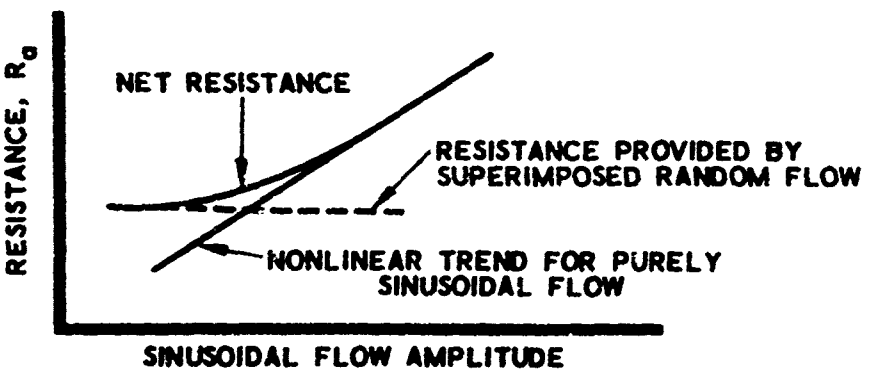

Fig. 18. Effect of Superimposed Random Flow on Accumulator Resistance

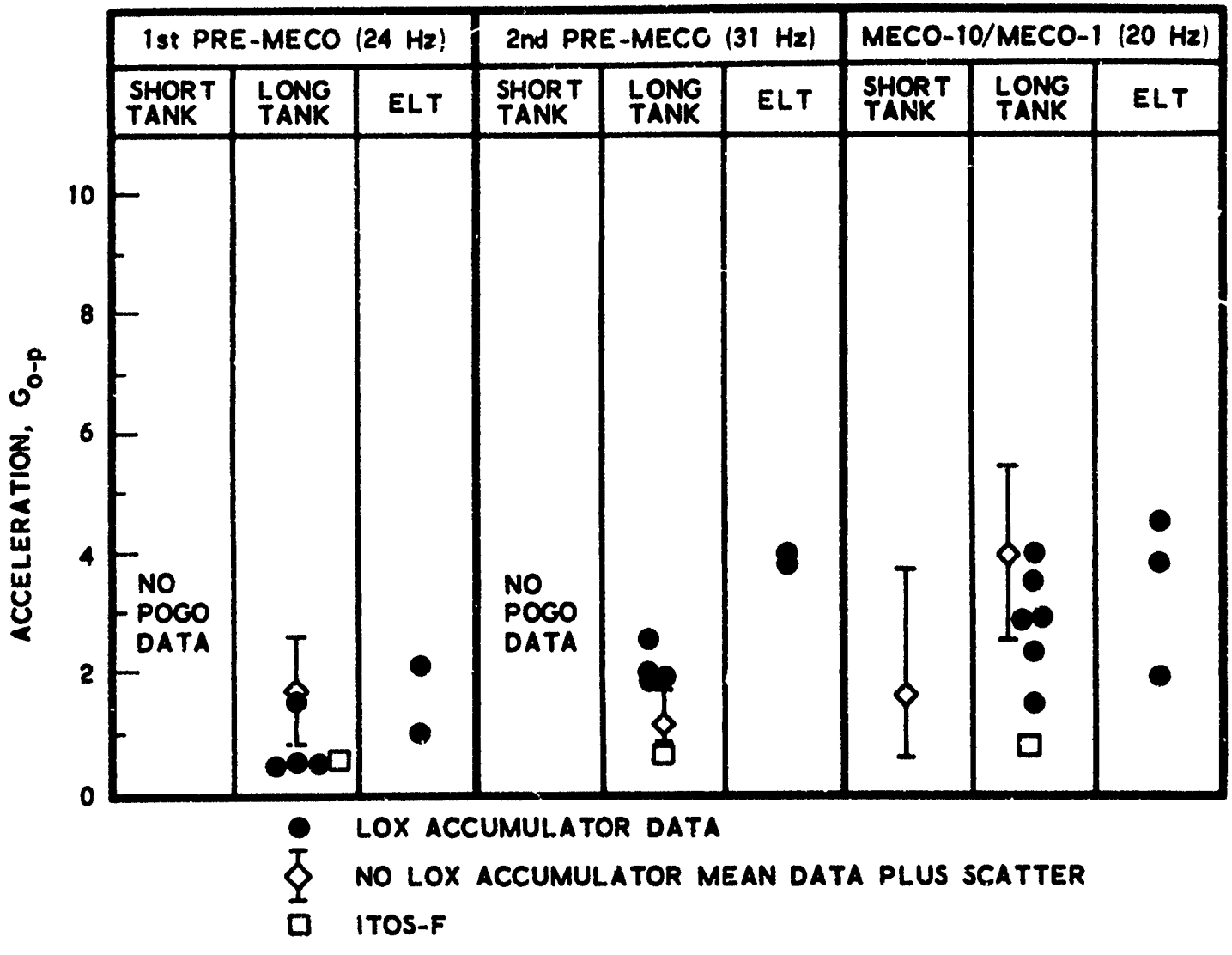

Fig. 19. Maximum Gimbal Block Accelerations for ITOS-F Relative to Other Delta Vehicles

SECTION VI

SUMMARY AND CONCLUSIONS

The reductions in pogo acceleration levels on the ITOS-F Vehicle were rendered possible by improvements in the quality of the mathematical stability model, which set the stage for the concept of a resistive lox accumulator. The improvement in the mathematical stability model has resulted from joint MDAC and Aerospace studies. The major Aerospace contributions are enumerated below.

1. The correction of the lox and fuel pump cavitation compliances. Detailed review of Thor/Agena Vehicle 344 data (Ref. 7) suggested that the fuel compliance was probably an order of magnitude higher than that previously provided by the engine contractor (Fig. 3). This was supported by subsequent estimation of the fuel compliance using the empirical method developed from data for the Saturn F-1, H-1, and J-2 pumps (Ref. 14). From a stability standpoint, the result was that the fuel contribution to the MECO pogo instability changed from significant to minor; consequently, MDAC halted consideration of a fuel accumulator. The empirical estimation method also provided new lox-pump cavitation compliances which were not substantially different from previously accepted values at low NPSH, but provided substantially greater values at high NPSH. This lox compliance change is therefore potentially significant for the early pogo events.

2. The detailed mathematical modeling of the lox and fuel feedlines by extension of the Titan feedline models (Ref. 11). The extensions accounted for the presence of elbows in both feedlines and the presence of the area change of the fuel feedline after it exits from the lox tank bottom. Moreover, the restudy of Vehicle 344 data also suggested that the fuel organ-pipe frequency was lower than previously assumed. A fuel-line modeling study showed that

the fuel bulk modulus would have to be below the range of published values to account for the flight observations. Use of the lower fuel bulk modulus was shown to be of significance for the first pogo event. This is believed to account for differences between Aerospace and MDAC stability results for this event. The acceptance by MDAC of the Aerospace discrete-parameter lox feedline model, in lieu of their representation with damped modes of the suction system, was essential to the proper consideration of the resistive accumulator.

3. The utilization of spectral analyses of flight data. In accord with Ref. 1, Aerospace recommended and MDAC performed cross-spectral analyses of pressure and acceleration data from as many flights as possible. Comparison of the resulting amplitude and phase relationship among the pressure and acceleration variables have been correlated with relationships from eigenvectors obtained from the stability analyses. This has led to new estimates of pump dynamic gains and the conclusion that the current mathematical model is adequate for the MECO stability event, but still inadequate for the two earlier events.

The modeling of the structural dynamics of the high-pressure discharge ducts by MDAC offers hope of explaining the pre-MECO pogo correlation. The measured resonant frequencies of the RS-27 discharge ducts during ground vibration tests appear to correlate with the instability frequencies. The flight instrumentation of these ducts, together with spectral reduction of the data, can be vital to an understanding of duct behavior and its role in the stability picture.

Understanding of the pogo stability situation on Delta vehicles has been greatly hampered by the lack of special-purpose dynamic testing of the propulsion system such as have been available for other vehicles (Ref. 1). In particular, it has only been possible to obtain correlatable data during the pogo events, and so the information is limited to the associated relatively

discrete frequencies for those events. It is unclear why the success achieved by Aerospace in analyses during the Titan vehicle Stage I flight in obtaining correlatable data fairly continuously over the entire flight (Fig. 10) has not been achieved for Delta flights. It may be significant that the Telesat data reduction, which used narrower, contiguous time slices, gave trends in all the eigenvector relationships consistent with stability analysis for the MECO event. Studies aimed at improving the data-reduction procedures should be carried out during analysis of data from future vehicles.

The corrected mathematical model showed that the MECO instability with an accumulator present resulted from a coincidence of the second lox feedline mode with the first longitudinal structural mode. The frequency of this second lox mode was very much dependent on the positioning of the accumulator relative to the pump, a distance equal to about one-third of the total feedline length. A significant raising of the second lox frequency by relocating the accumulator nearer to the pump was considered to be impractical because of the extensiveness of the hardware impact. The alternative proposed by Aerospace was to add resistance to the entry into the accumulator to increase the damping in the second lox mode. A preliminary criterion for optimization of the resistance was that the real part of the feedline flow impedance be maximized at the frequency of the second feedline mode. It was also shown that the inertance of orifices used to produce the resistance should be minimized; that is, a large number of small diameter holes is preferable to fewer larger holes. Subsequent stability analyses of the vehicle confirmed that the greatest stability improvement was indeed achieved for that value of resistance optimized via the feedline impedance approach.

The decision to implement an optimized resistive accumulator on the ITOS-E vehicle did not permit the recommended ground testing to investigate orifice resistance. Reliance was placed on resistance data from the testing of the Titan fuel accumulator (Ref. 15). The interpretation of this data was subsequently shown to be erroneous and resulted in an overly high resistance as demonstrated by the ITOS-E flight results (Fig. 2). The high resistance

produced an effective blocking of the accumulator and the ITOS-E pogo events were undistinguishable from those on a vehicle without an accumulator. Data reported in the literature, which came to light after the ITOS-E accumulator was configured, showed (1) that the majority of the Titan accumulator resistance must have been from something other than the presence of orifices, most probably from material dissipation within the rubber bladders or bladder rubbing, and (2) that the orifice resistance was nonlinear, with the value of resistance being proportional to the amplitude of flow oscillations. It was clear that sinusoidal testing was mandatory to investigate fluid viscosity effects, possible interaction among neighboring orifices, and the presence of random flow fluctuations. The basis for the test plan was developed by Aerospace and the tests were conducted by MDAC. There results the ITOS-F configuration of the resistance accumulator, having a total orifice area of 1.5 $in.^2$ as opposed to the 0.5 $in.^2$ for the ITOS-E configuration. The success of pogo suppression on the ITOS-F is displayed in Figs. 2 and 20.

After many years of major pogo instabilities on the Thor family of vehicles, a sufficient understanding has apparently been achieved resulting in an ability to suppress instabilities near MECO. Such understanding is still lacking for the earlier pogo events which suggests that it would be premature to discontinue the studies.

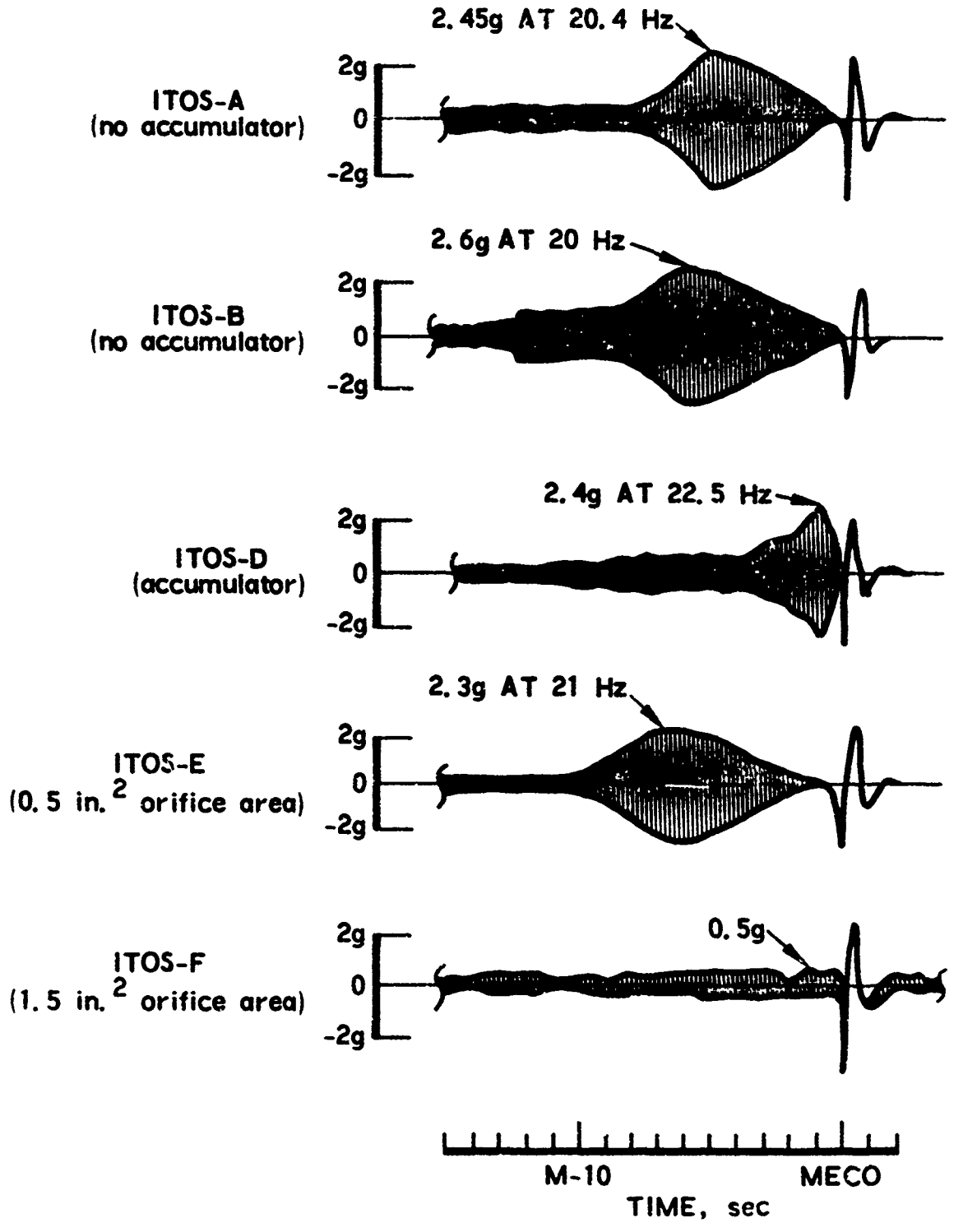

Fig. 20. Comparison of Guidance-Compartment Acceleration for Five ITOS Vehicles

REFERENCES

1. "Prevention of Coupled Structure - Propulsion Instability," NASA Space Vehicle Design Criteria (Structures), NASA SP-8055, October 1970.

2. "Final Technical Report, Thor Block 2 Test Program (20 cps Oscillation Problem)," R-3128, North American Aviation, Inc., August 1961.

3. Radovcich, N.A., "Analytical Model for Missile Axial Oscillation Induced by Engine-Structure Coupling," A658522, Lockheed Missiles and Space Company, March 1965.

4. Davis, W.F., T.F. Lynch, and T.R. Murray, "Thor 20 Cycle Longitudinal Oscillation Study," The Shock and Vibration Bulletin, 34(2), pp. 177-196, December 1964.

5. Woodward, G.B. and D.H. Gunderson, "Evaluation of High Compliance Device to Suppress 20 cps Longitudinal Oscillations in the Thor Vehicle," TER-65-2, North American Aviation, Inc., July 1965.

6. Davis, W.F., et al, "Feasibility Study of Compliant Devices to Eliminate Longitudinal Instability," SM-49005, Douglas Aircraft Company, August 1965.

7. "Summary Report, Development of a Longitudinal Oscillation Model for the Thor MB-3 Propulsion System," R-6337, North American Aviation, Inc., October 1965.

8. Lewis, W., "Simplified Analytical Model for Use in Design of Pump-Inlet Accumulators for the Prevention of Liquid-Rocket Longitudinal Oscillation (POGO)," NASA TN D-5394, 1969.

9. Wagner, R.G., "Titan II Engine Transfer Function Test Results," Report No. TOR-0059(6471)-9, The Aerospace Corporation, January 1971.

10. Rubin, S., "Instability Model of Missile Oscillation Due to Propulsion Feedback," Report No. TOR-269(4126)-28, The Aerospace Corporation, September 1964.

11. Payne, J.G., "Pogo Stability Analysis Program," Report No. TOR-0172 (2122)-10, The Aerospace Corporation, January 1972.

12. Rubin, S., R.G. Wagner, and J.G. Payne, "Pogo Suppression on Space Shuttle - Early Studies," NASA CR-2210, March 1973.

REFERENCES (Continued)

13. Leuner, T. R. and M. J. Morgan, "MB-3 Powered Long Tank and Extended Long Tank Delta Pogo Stability Analysis," A3-250-ABD3-73-TM-3, McDonnell Douglas Astronautics Company, May 1973.

14. Ghahremani, F. G. and S. Rubin, "Empirical Evaluation of Pump Inlet Compliance," Report No. ATR-73(7257)-1, The Aerospace Corporation, August 1972.

15. Zehnle, R., "T-III-M Phase 1A Frequency Response Test - Fuel Accumulator," TM 0472/20-2-68, Martin Marietta Corporation, June 1968.

16. Garrison, G. D., et al, "Suppression of Combustion Oscillations with Mechanical Damping Devices - Interim Report," PWA FR 3299, Pratt and Whitney Aircraft, August 1969.

17. Thurston, G. B. and C. E. Martin, "Periodic Fluid Flow Through Circular Orifices," J. A. S. A., 25(1), January 1953, p. 26.

18. Thurston, G. B., "Periodic Fluid Flow Through Circular Tubes," J. A. S. A., 24(6), November 1952, p. 653.

APPENDIX

CURRENT AEROSPACE POGO STABILITY EQUATIONS

Figure A-1 is a schematic representation of the Delta system followed by a current set of Aerospace stability equations. It should be pointed out that the subscript "o" is associated with fuel suction system variables and the subscript "f" with lox system variables. On the Titan vehicle, the fuel line is the short line represented incompressibly while the much longer oxidizer line is treated as compressible. The reverse is true for the Delta vehicle, i.e., the lox line is the shorter. However, the programs for the Titan had been written with variables subscripted "o" referring to that line represented as compressible, and this notation was maintained rather than reversing all the "o" and "f" subscripts. References 10 to 12 provide background information on the bases for the equations.

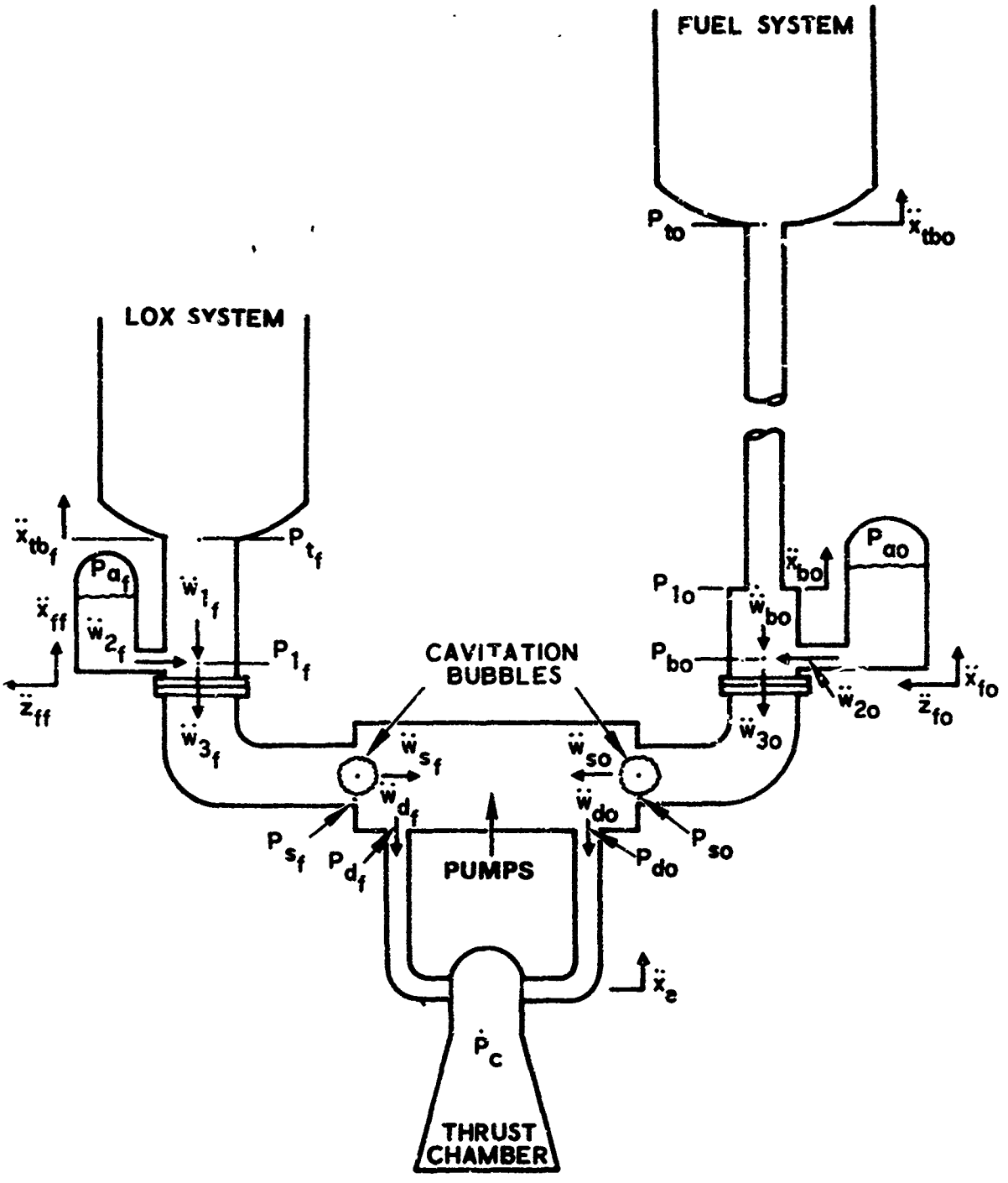

Fig. A-1. Schematic of Delta System

1. Modal Equation of Motion

$$\frac{s^2 + 2\zeta_i\omega_i s + \omega_i^2}{G_{ei}} \ddot{x}_{ei} - A_{lo}\left(\frac{p_{tboi}}{\phi_{ei}}\right)s^2\left(\sum_{j=1}^{M}\frac{\phi_{tboj}}{\phi_{ej}}\ddot{x}_{ej}\right)$$

$$-A_{sf}\left(\frac{p_{tbfi}}{\phi_{ei}}\right)s^2\left(\sum_{j=1}^{M}\frac{\phi_{tbfj}}{\phi_{ej}}\ddot{x}_{ej}\right) - \frac{\phi_{tboi}}{\phi_{ei}}A_{lo}s^2p_{to} - \frac{\phi_{tbfi}}{\phi_{ei}}A_{sf}s^2p_{tf}$$

$$-\left[\frac{1}{\rho_o}\frac{p_{tboi}}{\phi_{ei}}s + \left(\frac{\phi_{poxi}}{\phi_{ei}} + \frac{\phi_{pozi}}{\phi_{ei}}\right)A_{so}(R_{3Vo} + s\,L_{3Vo})\right]s\ddot{w}_{lo}$$

$$-\left[\frac{1}{\rho_f}\frac{p_{tbfi}}{\phi_{ei}}s + \left(\frac{\phi_{pfxi}}{\phi_{ei}} - \frac{\phi_{pfzi}}{\phi_{ei}}\right)A_{sf}(R_{3Vf} + s\,L_{3Vf})\right]s\ddot{w}_{lf}$$

$$-\left(\frac{\phi_{poxi}}{\phi_{ei}} + \frac{\phi_{pozi}}{\phi_{ei}}\right)A_{so}(R_{3Vo} + s\,L_{3Vo})\,s\ddot{w}_{2o}$$

$$-\left(\frac{\phi_{pfxi}}{\phi_{ei}} - \frac{\phi_{pfzi}}{\phi_{ei}}\right)A_{sf}(R_{3Vf} + s\,L_{3Vf})\,s\ddot{w}_{2f}$$

$$-\left[\frac{\phi_{tboi}}{\phi_{ei}}(A_{so} - A_{lo}) + \left(\frac{\phi_{poxi}}{\phi_{ei}} + \frac{\phi_{pozi}}{\phi_{ei}}\right)A_{so}\right]s^2p_{lo}$$

$$+\left(\frac{\phi_{pfxi}}{\phi_{ei}} - \frac{\phi_{pfzi}}{\phi_{ei}}\right)A_{sf}s^2p_{lf}$$

$$-\frac{\phi_{gi}}{\phi_{ei}}A_tC_fs^2p_c - \frac{\phi_{pozi}}{\phi_{ei}}A_{so}s^2p_{so} + \frac{\phi_{pfzi}}{\phi_{ei}}A_{sf}s^2p_{sf}$$

$$+\left[\frac{\phi_{tboi}}{\phi_{ei}}m_{lo}s - \left(\frac{\phi_{poxi}}{\phi_{ei}} + \frac{\phi_{pozi}}{\phi_{ei}}\right)\rho_oA_{so}(A_{lo} - A_{3o})(R_{3Vo} + s\,L_{3Vo})\right]s\ddot{x}_b$$

$$+\left(\frac{\phi_{poxi}}{\phi_{ei}}+\frac{\phi_{pozi}}{\phi_{ei}}\right)\rho_o A_{so}^2 R_{3Vo}\, s\left(\sum_{j=1}^{M}\frac{\phi_{poxj}}{\phi_{ej}}\ddot{x}_{ej}\right)$$

$$+\left(\frac{\phi_{pfxi}}{\phi_{ei}}-\frac{\phi_{pfzi}}{\phi_{ei}}\right)\rho_f A_{sf}^2 R_{3Vf}\, s\left(\sum_{j=1}^{M}\frac{\phi_{pfxj}}{\phi_{ej}}\ddot{x}_{ej}\right)=0$$

2. Engine Acceleration

$$\ddot{x}_e-\sum_{i=1}^{M}\ddot{x}_{ei}=0$$

3. Thrust Chamber

$$P_c-P_{co}-P_{cf}=0$$

4. Oxidizer Tank-Bottom Pressure

$$-L_{to}\ddot{w}_{lo}+\sum_{i=1}^{M}\left(\frac{P_{tboi}}{\phi_{ei}}-\rho_o A_{so}L_{to}\frac{\phi_{tboi}}{\phi_{ei}}\right)\ddot{x}_{ei}-p_{to}=0$$

5. Flow Continuity Across Oxidizer Pump

$$\rho_o A_{so}\left(\sum_{i=1}^{M}\frac{\phi_{poxi}}{\phi_{ei}}\ddot{x}_{ei}\right)-\ddot{w}_{lo}+\ddot{w}_{2o}+\rho_o A_{lo}-A_{so}\ddot{x}_{bo}$$

$$-\frac{s^2}{L_{so}\omega_{bo}^2}p_{so}-s\dot{w}_{do}=0$$

6. Incompressible Oxidizer Suction Line from Accumulator Location to Pump

$$sp_{bo} - sp_{so} - (R_{3o} + s\,L_{3o})\left[\ddot{w}_{1o} + \ddot{w}_{2o} + \rho_o(A_{1o} - A_{so})\ddot{x}_b\right]$$

$$- (R_{3o} + s\,L_{3Ho})\rho_o A_{so}\left(\sum_{i=1}^{M}\frac{\phi_{poxi}}{\phi_{ei}}\ddot{x}_{ei}\right)$$

$$- sL_{3Ho}\rho_o A_{so}\left(\sum_{i=1}^{M}\frac{\phi_{pozi}}{\phi_{ei}}\ddot{x}_{ei}\right) = 0$$

7. Oxidizer-Pump Performance

$$p_{do} - (m_o + 1)p_{so} + (R_{po} + s\,L_{po})\dot{w}_{do} = 0$$

8. Fuel Tank-Bottom Pressure

$$- L_{tf}\ddot{w}_{1f} + \sum_{i=1}^{M}\left(\frac{p_{tbfi}}{\phi_{ei}} - \rho_f A_{sf} L_{tf}\frac{\phi_{tbfi}}{\phi_{ei}}\right)\ddot{x}_{ei} - p_{tf} = 0$$

9. Flow Continuity Across Fuel Pump

$$\rho_f A_{sf}\left(\sum_{i=1}^{M}\frac{\phi_{pfxi}}{\phi_{ei}}\ddot{x}_{ei}\right) + \ddot{w}_{1f} + \ddot{w}_{2f} - \frac{s^2}{L_{sf}\omega_{bf}^2}{}_{sf} - s\dot{w}_{df} = 0$$

10. Incompressible Fuel Suction Line from Accumulator Location to Pump

$$sp_{1f} - sp_{sf} - (R_{3f} + s\,L_{3f})(\ddot{w}_{1f} + \ddot{w}_{2f})$$

$$- (R_{3f} + s\,L_{3Hf})\rho_f A_{sf}\left(\sum_{i=1}^{M}\frac{\phi_{pfxi}}{\phi_{ei}}\ddot{x}_{ei}\right) + s\,L_{3Hf}\rho_f A_{sf}\left(\sum_{i=1}^{M}\frac{\phi_{pfzi}}{\phi_{ei}}\ddot{x}_{ei}\right) = 0$$

11. Fuel-Pump Performance

$$p_{df} - (m_f + 1)p_{sf} + (R_{pf} + s\,L_{pf})\dot{w}_{df} = 0$$

12. Oxidizer-Accumulator Performance

$$s^2 p_{bo} + (L_{ao}s^2 + 2\zeta_{ao}\omega_{ao}L_{ao}s + L_{ao}\omega_{ao}^2)\ddot{w}_{2o} = 0$$

13. Fuel-Accumulator Performance

$$- \rho_f A_{4f} L_{4f} s^2 \sum_{i=1}^{M} \left(\frac{\phi_{pfxi}}{\phi_{ei}} \ddot{x}_{ei} \right) + s^2 p_{1f} + (L_{af}s^2 + 2\zeta_{af}\omega_{af}L_{af}s + L_{af}\omega_{af}^2)\ddot{w}_{2f} = 0$$

14. Flow in Fuel Suction Line from Tank Bottom to Accumulator Location

$$- sp_{tf} + sp_{1f} + (L_{1f}s + R_{1f})\ddot{w}_{1f} + \rho_f A_{sf} R_{1f} \ddot{x}_e = 0$$

15. Flow in Oxidizer Suction Line from Tank Bottom to Accumulator Location

$$- sp_{to} + sp_{1o} + \left(L_{1o}s + R_{1o} + \frac{\overline{\dot{W}}_o}{\rho_o g A_{1o}^2} \right) \ddot{w}_{1o} + \frac{1}{2} R_{1o} \rho_o A_{1o} \left[\ddot{x}_{bo} + \sum_{j=1}^{M} \frac{\phi_{tboj}}{\phi_{ej}} \dot{x}_{ej} \right] = 0$$

16. Flow in Oxidizer Discharge Line

$$p_{do} - p_c - (L_{do}s + R_{do})\dot{w}_{do} + \frac{\rho_o h_{do}}{g} \ddot{x}_e$$

17. Flow in Fuel Discharge Line

$$p_{df} - p_c - (L_{df}s + R_{df})\dot{w}_{df} + \frac{\rho_f h_{df}}{g}\ddot{x}_e$$

18.
19. Not used in Delta model

Feedline Equations

20. $$sp_{tom} - sp_{to} + \left(R_{1o} + \frac{\bar{w}_o}{\rho_o g A_{1o}^2}\right)\ddot{w}_{to} + \rho_o A_{1o} R_1 \ddot{x}_e = 0$$

21.
22. $$\begin{Bmatrix} p_{tom} \\ \ddot{w}_{to} \end{Bmatrix} = [T] \begin{Bmatrix} p_2 \\ \ddot{w}_{2oc} \end{Bmatrix}$$

23. $$sp_{2m} - sp_2 + R_2\ddot{w}_{2oc} + \rho_o A_{1o} R_2 \ddot{x}_e = 0$$

24.
25. $$\begin{Bmatrix} p_{2m} \\ \ddot{w}_{2oc} \end{Bmatrix} = [T] \begin{Bmatrix} p_3 \\ \ddot{w}_{3oc} \end{Bmatrix}$$

26. $$sp_{3m} - sp_3 + R_3\ddot{w}_{3oc} + \rho_o A_{1o} R_3 \ddot{x}_e = 0$$

27.
28. $$\begin{Bmatrix} p_{3m} \\ \ddot{w}_{3oc} \end{Bmatrix} = [T] \begin{Bmatrix} p_4 \\ \ddot{w}_{4oc} \end{Bmatrix}$$

29. $$sp_{4m} - sp_4 + R_4\ddot{w}_{4oc} + \rho_o A_{1o} R_4 \ddot{x}_e = 0$$

30.
31. $$\begin{Bmatrix} p_{4m} \\ \ddot{w}_{4oc} \end{Bmatrix} [T] \begin{Bmatrix} p_5 \\ \ddot{w}_{5oc} \end{Bmatrix}$$

32. $$sp_{5m} - sp_5 + R_5\ddot{w}_{5oc} + \rho_o A_{1o} R_5 \ddot{x}_e = 0$$

33.
34. $$\begin{Bmatrix} p_{5m} \\ \ddot{w}_{5oc} \end{Bmatrix} [T] \begin{Bmatrix} p_6 \\ \ddot{w}_{1o} \end{Bmatrix}$$

35. $$sp_{1o} - sp_6 + R_6\ddot{w}_{1o} + \rho_o A_{1o} R_6 \ddot{x}_e = 0$$

Feedline Model

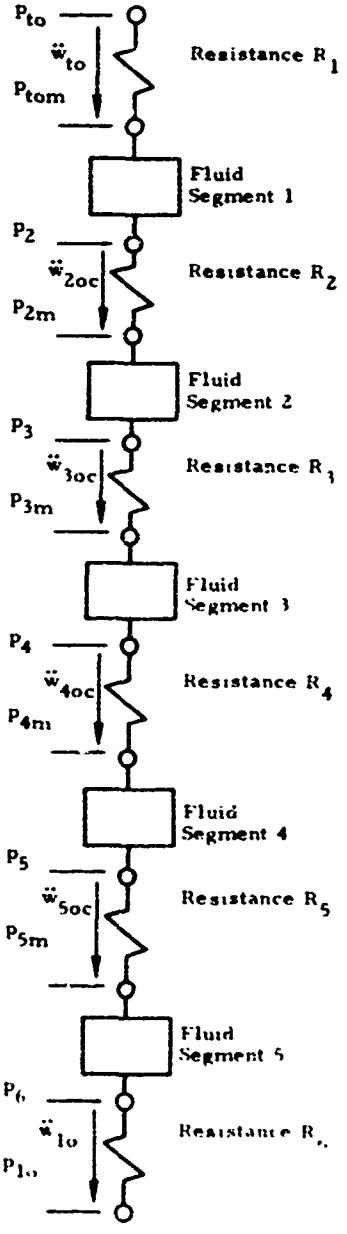

36. Oxidizer-Chamber Pressure

$$(1 + a_o s + \beta_o s^2) p_{co} - \frac{C_o^*}{A_t g} (1 + \gamma_o s + \delta_o s^2) \dot{w}_{do} = 0$$

37. Fuel-Chamber Pressure

$$(1 + a_f s + \beta_f s^2) p_{cf} - \frac{C_f^*}{A_t g} (1 + \gamma_f s + \delta_f s^2) \dot{w}_{df} = 0$$

38. Ox Feedline Section Between Area Change and Accumulator Location

$$sp_{lo} - sp_{bo} - \left[s L_{bo} + \left(R_{bo} + \frac{\bar{\dot{W}}_o}{\rho_o g A_{so}^2} \right) \right] \left[\ddot{w}_{lo} + \rho_o (A_{lo} - A_{so}) \ddot{x}_b \right]$$

$$- R_{bo} \rho_o A_{so} \ddot{x}_b + \frac{\bar{\dot{W}}_o}{\rho_o g A_{lo}^2} \ddot{w}_{lo} = 0$$

39. Equation of Motion for Ox Pipe in Section Between Tank and Area Change

$$\sum_{j=1}^{M} \frac{\phi_{tboj}}{\phi_{ej}} \ddot{x}_{ej} - \left(1 + \frac{m_{lo}}{2 k_{lo}} s^2 \right) \ddot{x}_{bo} + \frac{s^2}{k_{lo}} (A_{so} - A_{lo}) p_{lo} = 0$$

SYMBOLS

A	area ($in.^2$)
B	bulk modulus
C	compliance ($in.^2$)
K, k	spring rate (lb/in.)
L	inertance ($sec^2/in.^2$)
M, m	mass ($lb\text{-}sec^2/in.$)
P, p	pressure (psi)
R	resistance (sec/in.), real part of Z (sec/in.)
$\dot{W}, \dot{w}$	weight flow (lb/sec)
$\overline{\dot{W}}$	steady weight flow rate (lb/sec)
X	imaginary part of Z (sec/in.)
Z	impedance (sec/in.)
f	frequency (Hz)
g	acceleration in g's (ND), = 386 $in./sec^2$
h	acceleration change (in.)
m	dynamic pump gain-1
s	Laplace operator
x	longitudinal acceleration ($in./sec^2$)
y	lateral acceleration ($in./sec^2$)
z	lateral acceleration ($in./sec^2$)
$\alpha, \beta, \gamma, \delta$	constants in combustion equation
ζ	modal damping ratio (ND)

SYMBOLS (Continued)

ρ	weight density (lb/in.^{3})
ϕ	modal displacement shape (ND)
ω	circular frequency (rad/sec)

Subscripts

H	horizontal portion of section of line between accumulator and pump
V	vertical portion of section of line between accumulator and pump
a	accumulator
b	bubble
c	chamber
d	discharge
e	engine
f	lox
ff	lox line flange
fo	fuel line flange
i	refers to the i^{th} mode
o	fuel
p	pump
s	suction line, suction (pump inlet) conditions
t	tank
tb	tank bottom
1	section of suction line between tank and accumulator
3	section of suction line between accumulator and pump